

Reaction Rate Prediction via Group Additivity, Part 2: H-Abstraction from Alkenes, Alkynes, Alcohols, Aldehydes, and Acids by H Atoms

R. Sumathi, H.-H. Carstensen,[†] and William H. Green, Jr.*

Department of Chemical Engineering, Massachusetts Institute of Technology, 25 Ames Street, Cambridge, Massachusetts 02139

Received: May 14, 2001; In Final Form: July 9, 2001

The objective of this series of investigations is to develop procedures for predicting thermodynamically consistent generic rate rules for abstraction, addition, and isomerization reactions based on state-of-the-art quantum chemical calculations. This paper presents generic rate rules for H-abstraction from alkenes, alkynes, alcohols, aldehydes, and acids by hydrogen atoms. As described in detail in the first paper of this series {Sumathi, R.; Carstensen, H.-H.; Green, W. H., Jr. *J. Phys. Chem.*, in press}, we attempt to describe reaction rates in terms of group additivity. Analysis of ab initio computed transition structures of a series of molecules of a given reaction class reveals the existence of a nearly constant “reactive moiety”. We express thermodynamic contributions of these reactive moieties, which we refer to as “supergroups” since they contain several polyvalent atoms, to the entire transition state species in terms of group additivity values. The group additivity value of each “supergroup” is found to be transferable from one molecule to another within a given reaction family and is therefore identified as the characteristic of a given reaction class. The present study in combination with Benson’s group additivity tables allows prediction of reaction rates for 15 sets of reactions, which can be used as reasonable estimates in constructing large kinetic models. When available, we compare our estimates with literature data and find good or reasonable agreement. We also analyze the predicted thermodynamic properties for reactants and radicals to provide additional evidence for the reliability of the calculations. Some very small non-nearest-neighbor substituent effects are seen in the calculations, but these are generally too small to be easily discernible from experimental data.

Introduction

In the last two decades, considerable effort has been made to understand and model complex chemical reaction systems of industrial and environmental interest. A detailed model of any such system generally involves compilation of thousands of reactions including hundreds of reactive species. A major difficulty in developing such models is in obtaining information on the kinetic and mechanistic aspects of elementary reactions and estimating the relative contribution of competing product channels. The modelers preferably use experimental reaction rates whenever possible. However, all too often knowledge of reaction rate coefficients is needed at temperatures outside the range of preexisting experimental data. It is obvious that determining values for a large number of parameters by means of regression of experimental product distributions is both fundamentally undesirable and practically an impossible task. The huge quantity of kinetic data needed for modeling requires one to look for additional methods of estimation. An alternative way to obtain rate coefficients is through transition state theory. Benson,^{1a} in his thermochemical kinetics method, estimated the properties of a transition state by comparison with stable molecules and with model calculations of well-established rate constants. Cohen^{1b} extended the thermochemical kinetics formulation of conventional transition state theory to metathesis

reactions of H and OH with a series of alkanes to extrapolate rate coefficients to temperature regimes outside the range of experiments. Willems and Froment^{2–3} used transition state theory to obtain semiquantitative predictions for pre-exponential factors and activation energies. Similar to Benson’s work, the structure of transition states was guessed from chemical intuition. Although these models are still good and valid for qualitative predictions, the empirical origin of these models limits their applicability for quantitative predictions. With the advance of high performance computers and ab initio quantum chemical methods, it is now possible to calculate more reliable structural and energetic parameters, even for complex multi-channel reactions. This approach is conceptually preferable, owing to its rigorous quantum mechanical basis, and allows fairly accurate rate prediction for cases where empirical data are lacking.

In the first paper of this series,⁴ we introduced a concept based on ab initio calculations and group additivity (GA) to calculate and predict reactions rates within transition state theory (TST). We developed a procedure for calculating thermochemical properties of reasonable accuracy for stable molecules and transition states from quantum chemical calculations. We showed that the calculated geometrical parameters of the transition state specific moiety, “reactive moiety”, in the series of H-abstractions by H and CH₃ from alkanes remain nearly constant. The reaction lobe is thus hardly affected by structural changes in other parts of the molecule and can therefore be treated in terms of GA to contribute a nearly constant and transferable amount toward thermochemical properties of transition states. This allowed us

* To whom correspondence should be addressed. E-mail: whgreen@mit.edu. Fax: 001 617 252 1651.

[†] Present address: Chemical Engineering and Petroleum Refining Department, Colorado School of Mines, 329 Alderson Hall, Golden, CO 80401.

TABLE 1: List of Reactions Considered for the Derivation of Group Additivity Values (GAV) for Reactive Moieties in Transition States^a

“supergroup”	specific reactions	“supergr oup”	specific reactions
{CO/H/-H/H}	HCHO + H → HCO + H ₂	{Cd/H/- H/H}	CH₂=CH₂ + H → CH ₂ =CH + H ₂
{CO/C/-H/H}	MeCHO + H → MeCO + H ₂	“vinylic”	MeCH=CH₂ + H → MeCH=CH + H ₂
“aldehydic”	EtCHO + H → EtCO + H ₂		EtCH=CH₂ + H → EtCH=CH + H ₂
	i-PrCHO + H → i-PrCO + H ₂		i-PrCH=CH₂ + H → i-PrCH=CH + H ₂
	t-BuCHO + H → t-BuCO + H ₂		t-BuCH=CH₂ + H → t-BuCH=CH + H ₂
{O/C/-H/H}	MeOH + H → MeO + H ₂	{Cd/C/-H/H}	MeCH=CH₂ + H → MeC=CH ₂ + H ₂
“alcoholic”	EtOH + H → EtO + H ₂	“2° vinylic”	EtCH=CH₂ + H → EtC=CH ₂ + H ₂
	PrOH + H → PrO + H ₂		i-PrCH=CH₂ + H → i-PrC=CH ₂ + H ₂
	i-PrOH + H → i-PrO + H ₂		t-BuCH=CH₂ + H → t-BuC=CH ₂ + H ₂
	t-BuOH + H → t-BuO + H ₂		Me₂C=CH₂ + H → Me ₂ C=CH + H ₂
			CH₂=CHCH=CH₂ + H → CH ₂ =CHCH=CH + H ₂
{O/CO/-H/H}	HC(O)OH + H → HC(O)O + H ₂	{Ct/-H/H}	HCC + H → HCC + H ₂
“acid”	MeC(O)OH + H → MeC(O)O + H ₂	“alkynyl”	MeCCH + H → MeCC + H ₂
	PrC(O)OH + H → PrC(O)O + H ₂		EtCCH + H → EtCC + H ₂
	i-PrC(O)OH + H → i-PrC(O)O + H ₂		i-PrCCH + H → i-PrCC + H ₂
{C/Cd/H ₂ /-H/H}	CH₃CH=CH₂ + H → CH ₂ CHCH ₂ + H ₂	{C/Ct/H 2/-H/H}	CH₃CCH + H → CH ₂ CCH + H ₂
“allylic”		“propargylic”	
{C/Cd/C/H/-H/H}	MeCH₂CH=CH₂ + H → MeCHCH=CH ₂ + H ₂	{C/Ct/C/H/-H/H}	MeCH₂CCH + H → MeCHCCH + H ₂
“2° allylic”		“2° propargylic”	
{C/Cd/C ₂ /-H/H}	(Me)₂CHCH=CH₂ + H → (Me) ₂ CCH=CH ₂ + H ₂	{C/Ct/C 2/-H/H}	Me₂CHCCH + H → Me ₂ CCCH + H ₂
“3° allylic”		“3° propargylic”	
{C/Cd ₂ /H/-H/H}	(CH₂=CH)₂CH₂ + H → (CH ₂ =CH) ₂ CH + H ₂	{Cd/Ct/- H/H}	CH₂=CHCCH + H → CH ₂ =CCCH + H ₂
“diallylic”			
		{Cd/Cd/-H/H}	CH₂=CHCH=CH₂ + H → CH ₂ =CCH=CH ₂ + H ₂
			CH₂=CHC(Me)CH₂ + H → CH ₂ =CC(Me)CH ₂ + H ₂

^a We refer to these as “supergroups” because they contain more than one polyvalent atom.

to generalize the individual TST rates to a generic rate based on the group values for the reactive moiety. We refer to this moiety as “supergroup”, because it contains several polyvalent atoms and hence is not a group with respect to Benson’s definition.

We applied this methodology to investigate the prototypical bimolecular H-abstraction from the primary, secondary, and tertiary C–H bonds of alkanes by H and alkyl radicals for which experimental kinetic data are available. These data were for comparison in the 250–2000 K range.

In the present study, we extend our work to compute reaction rates for other types of H-abstraction reactions, especially from alkenes, alkynes, dienes, aldehydes etc., which are important intermediate constituents in the combustion of hydrocarbon fuels. For many of these systems it is experimentally difficult to determine the direct H-abstraction rates since alternative reaction paths (i.e., addition across the double or triple bond followed by isomerization and/or elimination), involving chemically activated intermediates are dominant at low temperatures and are still competitive at high temperatures. The reverse reactions often are difficult to measure as well, either because the reactions are significantly endothermic, or because the unsaturated radicals have competing reaction pathways. With the increasing use of automated reaction mechanisms for generating algorithms,^{5–17} there is an increasing need for kinetic information for all types of reactions. This is required to estimate their relative significance in a given reaction system. This work attempts to fill in some of the gaps.

The main objectives of this work are to extract GAVs for the reactive moiety (“supergroup” thermochemical value) in various H-abstractions by H from the families of alkenes, alkynes, dienes, alcohols, aldehydes, and acids. The different types of primary C–H bonds in alkanes, alkenes, and alkynes can be listed in terms of Benson’s group as {C/C/H₃}, {C/C_d/H₃}, and {C/C_t/H₃} while the secondary C–H bonds can have

six possible group representations based on simple permutation, i.e., {C/C₂/H₂}, {C/C/C_d/H₂}, {C/C/C_t/H₂}, {C/C_d²/H₂}, {C/C_t²/H₂}, and {C/C_d/C_t/H₂}. Similarly, the permutations of C(sp³), C_d(sp²) and C_t(sp) carbons in tertiary C–H bonds of hydrocarbons lead to 10 possibilities i.e., {C/C₃/H}, {C/C₂/C_d/H}, {C/C₂/C_t/H}, {C/C_d²/C_t/H}, {C/C_t²/C_d/H}, {C/C_d/C₂/H}, {C/C_t/C₂/H}, {C/C_d/C_t/H}, and {C/C_t/C₃/H}. The olefinic hydrogen in alkenes can be categorized as {C_d/H₂}, {C_d/C/H}, {C_d/C_d/H}, and {C_d/C_t/H} while the alkynic hydrogen belongs to the unique group {C_t/H}. The group values for the last two and seven groups, respectively, of the secondary and the tertiary C–H bonds (all shown in italic font in the above list) are not derived by Benson. Hence, out of the 24 possible C–H hydrogens in hydrocarbon families, Benson only characterized 15 groups and provided the thermochemical values for them. In our first paper, we derived “supergroup” GA values for three of them (primary, secondary, and tertiary C–H hydrogen abstractions), and herein we extend our work to the abstraction of the remaining 12 types of C–H hydrogen. The reactions considered for the derivation of the corresponding “supergroups” are tabulated in Table 1 along with a symbolic description of the reactive moiety. The abstracting hydrogen in each reaction is indicated in bold face italics.

In addition to the families of alkenes and alkynes, we also derive “supergroup” values for aldehydic (RCHO), acid (RCOOH), and alcoholic (ROH) hydrogens. We varied R from H, methyl, ethyl, and isopropyl to *tert*-butyl in each series. We have chosen these R substituents in order to see the effect of branching on the α position. Furthermore, the CO–H, O–H, and C_d–H bonds are relatively polar compared to the alkane C–H bond, therefore the bond strength of the abstracting bond can also be affected by the electronic effects of the R substituent. The computed reaction rates based on GA are compared with literature data whenever possible. In this paper, we present a set of 15 “supergroup” thermochemical values suitable for

predicting the H-abstraction rates from systems which are difficult to measure experimentally.

The remaining part of this paper is organized in the following way: First, we compare calculated thermodynamic properties of stable molecules with experimental values and predictions from group additivity. Although it was shown in the first paper of this series that the chosen level of ab initio calculation performs well in reproducing the experimental thermochemical values of saturated alkanes, it is essential to verify that the same is true with respect to the unsaturated, and therefore highly correlated, systems considered in this study. Furthermore, the GA values for these systems are less well determined and their reliability needs to be established. The derivation of GA values for the reactive moieties of the transition state species is based on Benson's GAV for the remaining parts of the molecules. Hence, it is important to have a good agreement between ab initio predicted and Benson's GA-estimated thermodynamic properties for stable molecules. After having shown the reliability of the calculations for the reactants, we turn to the transition states and derive the "supergroup" (reactive moiety) thermochemical values. Subsequently, we calculate reaction rates from group additivity values (GAV) and compare them with available experimental values and with the values in widely used kinetic models.

Calculation Procedure

In this work, quantum chemical calculations were employed to ascertain the structures and frequencies of transition states, reactants, and products. All calculations were carried out with the Gaussian 98 software package.¹⁸ Calculations were performed using the complete basis set model,¹⁹ CBS-Q, of Petersson et al. The method involves a series of calculations at the QCISD(T), MP4(SDQ), MP2 (with CBS extrapolation), and HF levels of theory with progressively larger basis sets. Further improvement with experimental data is achieved with an empirical correction and a correction for spin contamination. The spin correction term in the CBS-Q method is very significant for the present work as it accounts for errors resulting from the spin contaminated wave functions for open-shell systems within the UHF framework.

We adopt the commonly used procedure to calculate enthalpies of formation of molecules based on their atomization energies,²⁰ and experimental heats of formation ($\Delta H_f^{298\text{K}}$) for atoms. The enthalpies of formation thus obtained are further improved by incorporating the spin-orbit²¹ and bond-additivity corrections.²²

The total partition function of all species is calculated within the framework of the rigid-rotor-harmonic-oscillator approximation with corrections for internal rotation. As described in detail in ref 4, we use the MP2/6-31G(d') optimized geometrical parameters and HF/6-31G(d') computed, harmonic, vibrational frequencies scaled²³ by 0.91844 for the calculation of rotational and vibrational partition functions. All torsional motions about the single bonds between heavy atoms are treated as hindered internal rotations. The hindrance potential for the internal rotation is obtained at HF/6-31G(d') level by optimizing the 3N-7 internal coordinates, except the specific dihedral angle which characterizes the torsional motion. This dihedral angle is varied from 0 to 360° in increments of 20 degrees. The potential-energy surface thus obtained is then fitted to a Fourier series $\sum_m a_m \cos(m\phi) + b_m \sin(m\phi)$ with $m \leq 17$. Subsequently, the partition function for the hindered rotation is obtained by solving the Schrödinger equation for the energy eigenvalues with the fitted hindrance potential using the free rotor basis functions.

The partition function for hindered rotations is evaluated by direct counting, while the thermodynamic properties H, S, and Cp are calculated from the ensemble energy averages and fluctuations in internal energy, $\langle E \rangle^2$, and $\langle E^2 \rangle$. The exact treatment to obtain the hindered-rotor-partition function is discussed in detail in our first paper.⁴

The protocol to derive GAV of the "supergroup" from the thermochemical properties of transition states essentially stems from the assumption that the thermochemical contribution from the unreactive moiety in the transition state is nearly the same as in the reactants and is equal to that of Benson's group values. Consequently, GAV for reactive centers are derived by balancing the ab initio calculated $\Delta_R H^\ddagger$ (298.15 K), $\Delta_R S^\ddagger$ (298.15 K), and $\Delta_R C_p^\ddagger$ (Ts) of the reaction between the reactants and transition state (e.g., $\text{CH}_3\text{OH} + \text{H} \rightleftharpoons \text{CH}_3\text{O}\cdots\text{H}\cdots\text{H}$ (Transition state)) with those derived from Benson's group additivity table. The theoretically calculated heat of reaction ($\Delta_R H^\ddagger$) at 298 K for the formation of the transition state is given by

$$\Delta_R H^\ddagger(\text{calcd}) = \Delta_f H(\text{ts}) - \Delta_f H(\text{CH}_3\text{OH}) - \Delta_f H(\text{H}) = E_0 + \Delta H^{0 \rightarrow 298}(\text{ts}) - \Delta H^{0 \rightarrow 298}(\text{CH}_3\text{OH}) - \Delta H^{0 \rightarrow 298}(\text{H})$$

wherein $\Delta H^{0 \rightarrow 298}$ denotes the thermal contribution to the enthalpy at 298.15 K, E_0 is the energy difference between the reactants, $\text{CH}_3\text{OH} + \text{H}$, and the transition state at 0 K. The same $\Delta_R H^\ddagger$ value can also be obtained via group additivity

$$\begin{aligned} \Delta_R H^\ddagger &= \text{GA}(\text{ts}) - \text{GA}(\text{CH}_3\text{OH}) - \text{GA}(\text{H}) \\ &= H\{\text{C/O/H3}\} + H\{\text{O/C/-H/H}\} - H\{\text{C/O/H3}\} - H\{\text{O/C/H}\} - H\{\text{H}\} \\ &= H\{\text{O/C/-H/H}\} - H\{\text{H}\} - H\{\text{O/C/H}\} \end{aligned}$$

The notations $H\{\text{C/O/H3}\}$ and $H\{\text{O/C/H}\}$ represent Benson's heat of formation group values for CH_3O and OH moieties and $H\{\text{H}\}$ represents the group equivalent heat of formation for H radical. Finally, $H\{\text{O/C/-H/H}\}$ symbolizes the enthalpy associated with the reaction center $\text{O}\cdots\text{H}\cdots\text{H}$, which is defined in consistence with our earlier definition,⁴ and " $-\text{H}$ " symbolizes the migrating H atom. Balancing both expressions for $\Delta_R H^\ddagger$ together, we obtain the ΔH^{298} for the reaction center:

$$H\{\text{O/C/-H/H}\} = \Delta_R H^\ddagger(\text{calcd}) + H\{\text{O/C/H}\} + H\{\text{H}\}$$

Analogous formulas allow one to determine the intrinsic entropy (S_{int}^{298}) and the temperature-dependent $C_p(T)$ group additivity values for transition state "supergroups". However, in the case of intrinsic entropy, corrections for the symmetry (σ) of the reactants and transition state have to be taken into account, so that for the reaction of our example the following symmetry correction term is obtained.

$$S_{\text{int}}\{\text{O/C/-H/H}\} = \Delta_R S^\ddagger + S\{\text{O/C/H}\} + S\{\text{H}\} - R \ln(\sigma_{\text{CH}_3\text{OH}} \sigma_{\text{H}} / \sigma_{\text{ts}})$$

In contrast to our earlier work, herein we derive "supergroup" values by considering only the forward reaction resulting from the uncertainties, and missing thermochemical values for most of the radicals involved in the present study. The GA-predicted rate constant of a reaction is obtained by using the well-known transition state theory formula²⁴ and is corrected to account for tunneling using Wigner's perturbation theory formula²⁵

$$\kappa(T) = 1 + \frac{1}{24} \left(\frac{h\nu_i}{k_B T} \right)^2$$

where ν_i is the magnitude of the imaginary frequency of the reaction coordinate at the transition state.

Results and Discussion

The ab initio computed thermodynamic properties of the 30 stable molecules involved in the present study are tabulated in Tables 2 and 3 along with the experimental values and GA predictions. To compare with experimental data, we use the web-based NIST database.²⁶ However, for systems wherein, when we observed appreciable differences, we crosschecked with experimental values for stable molecules from Stull, Westrum, and Sinke.^{27a} For conjugated radicals from Orlov et al.^{27b} and Bozzelli et al.,²⁸ we have developed some additional group values to Benson's table, which will be of use in estimating the thermochemical values of some of the compounds investigated here. However, to ensure consistency we derive herein GAV for reactive centers based exclusively on Benson's table. We will discuss significant differences between GAV given by Benson and Therm at the appropriate places.

Thermochemical Properties of Stable Molecules

The stable molecules considered in this study fall into five major categories, i.e., alkenes, alkynes, aldehydes, acids, and alcohols, and here we analyze the results of Tables 2 and 3 within these broad classes.

Starting with the olefins and alkynes, we find that the ab initio predicted enthalpies of formation are usually within 1 kcal/mol of the empirical GA values, but in a few cases differences of up to 2.25 kcal/mol are seen. Agreement between GA and experimental values is significantly better. Given the amount of experimental data and their stated accuracy, it is very likely that the ab initio results are in error for this type of molecule. Petersson et al.²² also found that despite the introduction of bond additivity corrections (BAC) for C–C double and triple bonds, agreement with experimental values remained relatively poor. A possible explanation lies in the fact that the BAC for multiple bonds are derived from a mixed set of data including aromatic and other cyclic compounds, and that a more detailed differentiation of multiple bonds is required to adequately correct for systematic errors of CBS–Q. The same might hold for different types of C–H bonds, which are all, again, treated the same.

For the radicals derived from alkenes and alkynes, the experimental data are largely limited to heat of formation values and are often available only for conjugated allylic ($\text{CR}_2=\text{CR}-\text{CR}_2^*$) and propargylic ($\text{RCC}-\text{CR}_2^*$) type of radicals. The calculated ΔH_f^{298} values at the CBS–Q level for C_2H_3 and allyl radicals are, respectively, 71.59 and 40.85 kcal/mol. They are in excellent agreement with the NIST tabulated values of 71.50 and 40.90 kcal/mol. The experimental^{27b} ΔH_f^{298} value for but-1-ene-3-yl radical ($\text{CH}_2=\text{CHCH}^*\text{CH}_3$) is 30.40 ± 1.5 kcal/mol, while our calculated value after incorporating bond additivity and spin–orbit corrections is 31.57 kcal/mol, hence within the experimental uncertainty. O'Neal and Benson's^{27c} prediction for the heat of formation of 3-methylbut-1-ene-3-yl radical ($\text{CH}_2=\text{CHC}^*(\text{CH}_3)_2$) is 22.39 kcal/mol and correlates well with our calculated value of 22.47 kcal/mol. The experimental heat of formation of 1,4-pentadiene-3-yl radical ($\text{CH}_2=\text{CH}-\text{CH}^*-\text{CH}=\text{CH}_2$) is 48.99 kcal/mol with a very large uncertainty of 3.1 kcal/

mol and our calculated value (46.18 kcal/mol) is in accord with its lower bound.

In summary, ab initio calculated ΔH_f s agree with experiment and literature GA estimates to better than 0.6 kcal/mol in every case except 3,3-dimethylbutene, 1,3-butadiene, and 1,4-pentadiene. There are substantial discrepancies in the literature ΔH_f values for 3,3-dimethylbutene and vinylacetylene. The group additivity value for $\Delta H_f^{(298\text{K})}$ of $\{\text{C}_i/\text{C}_a\}$ group in vinylacetylene differs by 1 kcal/mol between Benson's table^{1a} (29.2 kcal/mol) and the THERM²⁸ value (28.2 kcal/mol), with the former agreeing better with experimental and ab initio data. Ab initio entropies are generally accurate to 0.5 cal/mol-K. In the case of the $\{\text{C}/\text{C}_2/\text{H}_2\}$ group, as encountered in 1,4-pentadiene, better agreement is observed with Benson's^{1a} S^{298} value (10.2 cal/mol-K) compared to the 8.13 cal/mol-K value from THERM.²⁸ Ab initio heat capacities are generally accurate to 0.5 cal/mol-K.

In the series of alcohols, except for *tert*-butyl alcohol, ab initio predicted ΔH_f s are within 0.2 kcal/mol of the literature and GA predictions. The ΔH_f for *tert*-butyl alcohol differs by nearly 1 kcal/mol but this discrepancy is small compared to the broad range of experimentally derived values quoted in the literature. The ab initio result lies between the experimental values. The S^{298} and Cp(T) values are well predicted and are in agreement within ± 0.3 cal/mol-K. Not much is known experimentally about the thermochemistry of alkoxy radicals except for methoxy. The experimental heat of formation of the methoxy radical at 298 K is 4.1 ± 1.0 kcal/mol while the calculated value is 5.4 kcal/mol, near the upper bound of the experimental data. It is appropriate to mention the recent investigations on enthalpies of formation of alcohols and ethers by DeTar²⁹ based on formal steric enthalpy values computed at the MP2/6-31+G-(d,p)//6-31G(d,p) level which obtained a standard deviation of 0.56 kcal/mol with a maximum deviation of 1.35 kcal/mol.

In the case of aldehydes, ab initio calculated heats of formation are in very good agreement with GA predictions and differ by at most 1 kcal/mol with experimental results. Also, the computed $\Delta H_f^{(298\text{K})}$ for formyl and acetyl radicals (10.26 and -2.3 kcal/mol, respectively) are in excellent agreement with literature values (10.4 and -2.9 kcal/mol, respectively). The NIST-tabulated heats of formation for HCHO and CH_3CHO differ significantly from Pedley's^{27d} experimental values ($\Delta H_f(\text{HCHO}) = -25.96$ kcal/mol and $\Delta H_f(\text{CH}_3\text{CHO}) = -39.70$ kcal/mol). In the case of *t*-BuCHO, GA-predicted ΔH_f does not match with our ab initio value. The lack of reliable experimental data makes it difficult to identify the source of this problem. Additional work is needed. The S values are reproduced within ± 0.15 cal/(mol-K). Cp(T) values for HCHO, CH_3CHO , and $\text{CH}_3\text{CH}_2\text{CHO}$ are in excellent agreement (within a few tenths of one cal/(mol-K)) with GA values. Cp(T) values for $\{\text{C}/\text{C}_2/\text{CO}\}$ and $\{\text{C}/\text{C}_3/\text{CO}\}$ groups are not given in Benson's compilation, but these groups are available in THERM software.²⁸ However, use of these group values to evaluate Cp(T)s for *i*-PrCHO and *t*-BuCHO shows a mismatch between GA and ab initio predictions of up to 1 cal/(mol-K) at high temperatures. Additional experimental results are needed to resolve the correctness of either the ab initio or the GA data.

As shown in Table 2, the enthalpies of formation and entropies of acids are reproduced within 0.5 kcal/mol and 0.5 cal/mol-K, respectively. However, the S^{298} values for the $\{\text{CO}/\text{C}/\text{O}\}$ group used by Benson^{1a} (14.8 cal/mol-K) and THERM²⁸ (10.4 cal/mol-K) differ appreciably. Within the limited set of acids investigated in this study, the observed agreement in Table 2 for S^{298} suggests that Benson's GA value for this group is

TABLE 2: Comparison of Calculated Thermodynamic Properties of Alkenes and Alkynes with Group Additivity (GA) Predictions^{1a} and Experimental Data^b

species	source	$\Delta_f H^{298}$	S^{298}	C_p^{300}	C_p^{400}	C_p^{500}	C_p^{600}	C_p^{800}	C_p^{1000}	C_p^{1500}
CH ₂ =CH ₂	ab initio	13.1	52.3	10.12	12.44	14.67	16.63	19.81	22.25	26.16
	SWS	12.5	52.5	10.45	12.90	15.16	17.10	20.20	22.57	—
	GA[Benson]	12.5	52.5	10.20	12.72	15.02	17.00	20.14	22.54	26.38
	NIST	12.5	52.4	10.30	12.68	14.93	16.89	20.03	22.44	26.28
CH ₃ CH=CH ₂	ab initio	5.4	63.6	15.25	18.94	22.42	25.48	30.47	34.27	40.27
	SWS	4.9	63.8	15.34	19.10	22.62	25.70	30.68	34.46	—
	GA[Benson]	4.7	63.8	15.45	19.23	22.72	25.79	30.74	34.49	40.39
	NIST	4.9	63.8	15.44	19.23	22.75	25.81	30.77	34.52	40.44
CH ₃ CH ₂ CH=CH ₂	ab initio	0.4	73.0	20.69	25.95	30.77	34.93	41.60	46.64	54.55
	SWS	0.0	73.0	20.57	26.04	30.93	35.14	41.80	46.82	—
	GA[Benson]	0.1	73.5	20.61	26.17	31.08	35.28	41.98	46.98	54.78
	NIST	-0.2	73.1	20.55	25.93	30.85	35.07	41.80	46.85	54.71
(CH ₃) ₂ CHCH=CH ₂	ab initio	-6.9	79.4	27.24	33.79	39.76	44.90	53.10	59.28	68.96
	SWS	-6.9	79.7	28.47	35.26	40.97	45.90	53.85	59.83	—
	GA[Benson]	-6.6	80.1	25.88	33.14	39.54	44.77	53.26	59.47	69.31
	NIST	-6.5	79.7	27.50	34.20	40.20	45.41	53.50	59.80	69.30
(CH ₃) ₃ CCH=CH ₂	ab initio	-15.7	83.2	32.24	40.89	48.52	54.92	64.87	72.20	83.57
	SWS	-10.3	82.2	30.39	38.90	46.70	53.40	63.60	71.00	—
	GA[Benson]	-13.5	83.0	31.94	41.19	49.07	55.63	65.76	73.02	83.87
	NIST	-14.5	82.2	—	—	—	—	—	—	—
(CH ₃) ₂ C=CH ₂	ab initio	-3.3	69.9	21.10	26.13	30.74	34.79	41.40	46.47	54.45
	SWS	-4.0	70.2	21.39	26.57	31.24	35.30	41.86	46.85	—
	GA[Benson]	-3.8	70.0	21.58	26.65	31.30	35.34	41.91	46.89	54.71
	NIST	-4.3	70.2	21.15	26.24	30.92	35.01	41.66	46.71	54.63
(CH ₃) ₂ C=CH(CH ₃)	ab initio	-10.4	80.3	25.36	31.51	37.44	42.73	51.42	58.02	68.32
	SWS	-10.2	80.9	25.22	31.93	38.07	43.42	52.05	58.55	—
	GA[Benson]	-10.7	80.0	25.49	32.07	38.19	43.52	52.12	58.58	68.72
	NIST	-9.9	80.9	25.22	31.93	38.07	43.42	52.05	58.55	68.63
(CH ₂ =CH) ₂ CH ₂	ab initio	26.7	80.0	24.87	30.18	35.18	39.53	46.52	51.78	60.02
	SWS	25.2	79.7	25.20	31.30	36.50	40.80	47.60	52.70	—
	GA[Benson]	25.4	80.0	23.22	29.58	35.04	39.60	46.74	52.04	60.02
	NIST	25.4	79.8	23.60	30.09	35.83	40.66	48.16	53.61	62.00
CH ₂ =CHCH=CH ₂	ab initio	27.7	65.9	18.66	24.18	28.75	32.28	37.30	40.87	46.47
	SWS	26.3	66.6	19.11	24.29	28.52	31.84	36.84	40.52	—
	GA[Benson]	26.1	66.6	19.12	24.30	28.52	31.84	36.84	40.52	46.34
	NIST	26.0	66.6	19.18	24.72	29.18	32.63	37.68	41.37	47.21
CH ₂ =CHC(CH ₃)=CH ₂	ab initio	18.5	75.1	25.06	31.84	37.23	41.47	47.92	52.74	60.44
	SWS	18.1	75.4	25.20	31.80	37.10	41.40	48.00	52.90	—
	GA[Benson]	18.0	75.2	25.25	31.72	37.10	41.39	48.01	52.92	60.66
	NIST	18.1	75.2	24.67	30.97	36.37	40.88	47.94	53.18	61.23
CH ₂ =CHCCH	ab initio	69.2	66.0	16.86	20.57	23.62	26.10	29.93	32.78	37.28
	SWS	72.8	66.8	17.57	21.26	24.25	26.67	30.40	33.16	—
	GA[Benson]	69.2	66.8	17.40	21.68	24.25	27.71	31.23	33.72	37.80
	NIST	70.4	66.8	17.57	21.26	24.25	26.67	30.40	33.16	—
HCCH	ab initio	55.6	47.6	10.00	11.54	12.66	13.52	14.87	15.94	17.82
	SWS	54.2	48.0	10.53	11.97	12.97	13.73	14.93	15.92	—
	GA[Benson]	53.9	48.0	10.54	11.98	12.98	13.74	14.94	15.92	17.66
	NIST	54.2	48.0	10.56	12.04	13.09	13.89	15.18	16.24	18.18
CH ₃ CCH	ab initio	43.6	58.8	14.16	16.95	19.38	21.47	24.87	27.50	31.71
	SWS	44.3	59.3	14.55	17.33	19.74	21.80	25.14	27.71	—
	GA[Benson]	44.3	59.3	14.59	17.31	19.70	21.75	25.09	27.65	32.76
	NIST	44.3	59.3	14.57	17.34	19.74	21.80	25.15	27.73	31.86
CH ₃ CH ₂ CCH	ab initio	39.1	68.7	19.14	23.66	27.52	30.77	35.92	39.82	45.96
	SWS	39.5	69.5	19.54	23.87	27.63	30.83	35.92	39.84	—
	GA[Benson]	39.8	69.5	19.58	23.95	27.67	30.83	35.97	39.85	46.99
	NIST	39.5	69.6	19.64	24.06	27.87	31.08	36.19	40.05	46.13
(CH ₃) ₂ CHCCH	ab initio	31.4	75.6	24.87	31.00	36.24	40.59	47.38	52.45	60.38
	SWS	32.6	76.2	25.13	31.10	36.20	40.60	47.40	52.40	—
	GA[Benson]	32.8	76.1	24.85	30.92	36.03	40.32	47.25	52.34	61.52
	NIST	32.6	76.3	25.48	31.46	36.54	40.78	47.49	52.53	60.44

^a $\Delta_f H^{298}$ is given in kcal/mol, S^{298} and $C_p(T)$ data are in cal/(mol*K). The calculated properties are given for the most stable conformer. ^b NIST = NIST Webook^{26a} or NIST Standard Reference Database 25.^{26b}

more accurate. $C_p(T)$ values at high temperature follow the trend NIST > ab initio > GA, and the maximum difference between NIST and GA is approximately 1 cal/mol-K. This shows that ab initio predictions are very reliable.

Structure and Properties of the Transition State

The optimized geometries, vibrational frequencies, and moments of inertia of the 40 transition states studied in the present

work are given in the Supporting Information. The characteristic geometric parameters of the reactive moieties, i.e., the breaking Y-H and forming H-H bond distances and the associated bond angle, are tabulated in Table 4. It also contains the magnitude of the imaginary frequency corresponding to the reaction coordinate at the transition states and the expectation value of spin operator, $\langle S^2 \rangle$, for the transition states of all reactions. The $\langle S^2 \rangle$ value is a measure of the extent of spin contamination

TABLE 3: Comparison of Calculated Thermodynamic Properties of Alcohols, Aldehydes and Acids with Group Additivity (GA) Predictions^{1a} and Experimental Data^b

species	source	$\Delta_f H^{298}$	S^{298}	c_p^{300}	c_p^{400}	c_p^{500}	c_p^{600}	c_p^{800}	c_p^{1000}	c_p^{1500}
HCHO	ab initio	-26.3	52.1	8.41	9.25	10.28	11.31	13.14	14.59	16.84
	SWS	-27.7	52.3	8.47	9.38	10.46	11.52	13.37	14.81	—
	GA [Benson]	-26.0	52.3	8.47	9.38	10.46	11.52	13.37	14.80	17.00
	NIST	-27.7	52.3	8.47	9.38	10.45	11.52	13.37	14.81	17.01
CH ₃ CHO	ab initio	-39.5	62.9	12.91	15.34	17.78	20.00	23.70	26.51	30.86
	SWS	-39.8	63.2	13.11	15.73	18.27	20.52	24.20	26.96	—
	GA[Benson]	-39.2	63.1	13.19	15.64	18.20	20.49	24.22	26.97	—
	NIST	-40.8	63.2	13.27	15.84	18.33	20.54	24.16	26.89	31.09
CH ₃ CH ₂ CHO	ab initio	-44.5	72.7	19.70	22.95	26.32	29.45	34.71	38.75	45.05
	SWS	-45.9	72.8	18.87	23.09	26.89	30.22	35.45	39.27	—
	GA[Benson]	-44.3	72.6	19.43	23.42	26.94	29.99	35.34	39.18	—
	NIST	-45.1	72.8	19.35	23.04	26.98	30.71	37.09	42.14	50.60
(CH ₃) ₂ CHCHO	ab initio	-51.5	79.6	24.43	29.67	34.56	38.85	45.83	51.11	59.32
	GA[Benson]	-50.8	79.1	—	—	—	—	—	—	—
	NIST	-51.6	79.4	—	—	—	—	—	—	—
(CH ₃) ₃ CCHO	ab initio	-60.2	83.9	29.46	36.73	43.17	48.65	57.31	63.76	73.75
	GA[Benson]	-57.7	84.1	—	—	—	—	—	—	—
	NIST	—	—	—	—	—	—	—	—	—
HC(O)OH	ab initio	-90.3	59.3	10.76	12.72	14.58	16.26	18.99	20.97	23.54
	SWS	-90.5	59.5	10.84	12.85	14.62	16.02	18.35	19.95	—
	GA[Benson]	-90.2	59.4	10.80	12.90	14.60	16.00	18.40	20.00	—
	NIST	-90.5	59.4	10.96	13.03	14.97	16.68	19.44	21.37	23.67
CH ₃ C(O)OH	ab initio	-103.2	68.0	15.43	18.91	22.07	24.83	29.33	32.72	37.61
	SWS	-103.9	67.5	15.97	19.52	22.60	25.15	29.08	31.99	—
	GA[Benson]	-103.3	67.5	15.99	19.54	22.50	25.09	29.12	31.97	—
	NIST	-103.3	67.6	15.23	19.04	22.45	25.38	30.00	33.28	37.67
CH ₃ CH ₂ C(O)OH	ab initio	-108.4	77.3	21.79	26.23	30.45	34.20	40.35	44.98	51.78
	GA[Benson]	-108.4	77.0	22.23	27.32	31.24	34.59	40.24	44.18	—
	NIST	-107.0	77.1	—	—	—	—	—	—	—
	(CH ₃) ₂ CHC(O)OH	ab initio	-115.3	84.2	26.85	33.27	39.00	43.90	51.69	57.51
(CH ₃) ₃ COH	GA[Benson]	-114.9	83.5	—	—	—	—	—	—	—
	NIST	-115.0	83.8	—	—	—	—	—	—	—
	ab initio	-48.0	57.1	10.59	12.29	14.16	15.92	18.90	21.24	25.06
CH ₃ OH	SWS	-48.1	57.3	10.52	12.29	14.22	16.02	19.04	21.38	—
	GA[Benson]	-48.0	57.3	10.49	12.24	14.20	15.99	19.02	21.37	—
	NIST	-48.1	57.3	10.56	12.34	14.27	16.06	19.06	21.40	25.19
	ab initio	-56.0	66.8	15.75	19.21	22.52	25.43	30.12	33.70	39.39
CH ₃ CH ₂ OH	SWS	-56.1	67.5	15.71	19.36	22.77	25.69	30.33	33.83	—
	GA[Benson]	-56.0	67.0	15.52	19.17	22.54	25.42	30.15	33.71	—
	NIST	-56.2	67.5	15.65	19.41	22.89	25.87	30.57	34.10	39.68
	ab initio	-61.1	76.1	20.85	25.90	30.62	34.71	41.21	46.07	53.71
CH ₃ CH ₂ CH ₂ OH	SWS	-61.6	77.6	20.91	25.86	30.51	34.56	41.04	45.93	—
	GA[Benson]	-61.0	76.4	21.02	26.14	30.78	34.76	41.23	46.05	—
	NIST	-61.1	77.1	20.54	25.82	30.64	34.75	41.26	46.12	53.76
	ab initio	-65.4	73.9	21.70	26.75	31.35	35.29	41.56	46.28	53.77
(CH ₃) ₂ CHOH	SWS	-65.2	74.1	21.31	26.78	31.89	35.76	42.13	46.82	—
	GA[Benson]	-65.1	74.3	21.56	26.88	31.78	35.51	41.89	46.56	—
	NIST	-65.2	74.1	21.45	26.80	31.54	35.44	41.36	45.64	52.28
	ab initio	-75.9	77.9	27.76	34.57	40.58	45.62	53.45	59.25	68.38
(CH ₃) ₃ COH	SWS	-77.9	78.0	27.23	34.16	40.27	45.37	53.32	59.16	—
	GA[Benson]	-74.5	77.7	27.32	34.35	40.37	45.27	53.32	59.18	—
	NIST	-74.7	78.0	27.29	34.18	40.25	45.33	53.23	59.10	68.27

^a $\Delta_f H^{298}$ is given in kcal/mol, S^{298} and $C_p(T)$ data are in cal/(mol*K). The calculated properties are given for the most stable conformer. ^b NIST = NIST Webook^{26a} or NIST Standard Reference Database 25.^{26b}

in the UHF wave function. As can be observed, several of the transition structures are spin contaminated, with $\langle S^2 \rangle$ being significantly greater than 0.75, the expected value for a pure-doublet state. The empirical spin correction term included in the CBS-Q method, i.e., $-9.2 * \Delta \langle S^2 \rangle$ where $\Delta \langle S^2 \rangle$ is the difference between the spin expectation value of the contaminated wave function and that of its pure eigenstate, always lowers the energy of the barrier since $\Delta \langle S^2 \rangle$ is always positive. It is interesting to note that the $\langle S^2 \rangle$ value remains nearly constant for a particular reaction set. Consequently, even if the spin correction term does not completely recover the true energy, the error in the barrier height should be about the same for the entire series.

The geometry of the reactive moiety, i.e., the lengths of the abstracting Y-H and the newly forming H-H bonds, and the angle between them, remains nearly the same throughout the chosen set of reactions. Recently, other investigators such as Masel et al.^{30a} and Troung et al.,^{30b} have also reported the near constancy of the reactive moiety in the transition states of H-abstraction using different levels of quantum chemical calculations. As can be observed in Table 4, the bond distances agree in most cases up to the second decimal value. However, this does not hold for all types of reactions. One exception is the series of RO-H, RC(O)-H abstractions: the abstracting C(O)-H bond at the transition state tends to be longer (by approximately 0.1Å) for R = t-Bu compared to R = CH₃. From

TABLE 4: The MP2/6-31G(d') Optimized Bond Distances (in Å) and Bond Angles (in Degrees) of the Reactive Moiety in the Transition Structures along with the Magnitude of the Imaginary Frequency^a

transition structure	Y-H	H-X	Y-H-X	$\langle S^2 \rangle$	ν in cm^{-1}	barrier
CH ₃ OH + H	1.235	0.875	171.2	0.794	3400	12.32
CH ₃ CH ₂ OH + H	1.242	0.873	171.5	0.794	3384	12.51
CH ₃ CH ₂ CH ₂ OH + H	1.241	0.873	171.7	0.794	3385	12.30
(CH ₃) ₂ CHOH + H	1.243	0.873	172.7	0.794	3387	12.25
(CH ₃) ₃ COH + H	1.248	0.874	174.3	0.794	3381	11.86
HCHO + H	1.329	0.999	179.4	0.808	2476	4.79
CH ₃ CHO + H	1.334	0.998	179.1	0.796	2389	3.30
CH ₃ CH ₂ CHO + H	1.337	0.997	178.8	0.796	2382	2.96
(CH ₃) ₂ CHCHO + H	1.338	0.998	178.6	0.795	2370	2.62
(CH ₃) ₃ CCHO + H	1.341	0.999	179.3	0.795	2363	2.22
HC(O)OH + H	1.338	0.829	173.2	0.791	3191	16.11
CH ₃ C(O)OH + H	1.332	0.830	174.3	0.791	3241	16.72
CH ₃ CH ₂ C(O)OH + H	1.332	0.831	174.6	0.791	3243	16.28
(CH ₃) ₂ CHC(O)OH + H	1.325	0.835	174.7	0.792	3245	15.25
CH ₂ =CH ₂ + H	1.467	0.854	176.5	0.922	2140	13.75
CH ₃ -CH=CH ₂ + H	1.477	0.850	176.5	0.912	2116	13.89
CH ₃ CH ₂ CH=CH ₂ + H	1.477	0.851	176.6	0.909	2118	13.77
(CH ₃) ₂ CHCH=CH ₂ + H	1.478	0.851	176.7	0.903	2118	13.59
(CH ₃) ₃ CCH=CH ₂ + H	1.475	0.852	176.7	0.904	2124	13.48
(CH ₃) ₂ C=CH ₂ + H	1.489	0.849	179.7	0.903	2100	13.94
CH ₂ =CH-CH=CH ₂ + H	1.471	0.851	176.6	1.130	2122	14.18
CH ₃ CH=CH ₂ + H	1.452	0.866	177.5	0.901	2165	10.92
CH ₃ CH ₂ CH=CH ₂ + H	1.457	0.866	177.2	0.898	2155	10.80
(CH ₃) ₂ CHCH=CH ₂ + H	1.457	0.866	177.0	0.895	2158	10.53
(CH ₃) ₃ CCH=CH ₂ + H	1.461	0.866	176.2	0.894	2154	10.27
(CH ₃) ₂ C=CCH ₃ H + H	1.467	0.863	177.8	0.892	2141	10.17
CH ₃ CH=CH ₂ + H	1.356	0.928	177.5	0.927	2388	5.52
CH ₃ CH ₂ CH=CH ₂ + H	1.351	0.933	176.6	0.910	2315	3.51
(CH ₃) ₂ CHCH=CH ₂ + H	1.331	0.935	176.6	0.887	2262	2.20
(CH ₂ =CH) ₂ CH ₂ + H	1.331	0.951	177.6	1.005	2286	1.15
HCC-CH ₃ + H	1.440	0.864	179.9	0.873	2441	8.30
HCC-CH ₂ CH ₃ + H	1.384	0.902	178.3	0.863	2452	4.18
HCC=CH(CH ₃) ₂ + H	1.371	0.911	179.2	0.853	2393	1.22
CH ₂ =CHCH=CH ₂ + H	1.466	0.858	176.2	1.087	2156	12.15
CH ₂ =CHC(CH ₃)=CH ₂ + H	1.469	0.857	175.5	1.045	2156	12.04
CH ₂ =CH-CCH + H	1.450	0.858	176.0	1.122	2341	8.28
HCCH + H	1.670	0.781	179.6	1.052	1598	28.88
CH ₃ CCH + H	1.669	0.782	179.9	1.025	1603	28.48
CH ₃ CH ₂ CCH + H	1.669	0.782	179.9	1.024	1606	28.04
(CH ₃) ₂ CHCCH + H	1.671	0.782	179.9	1.023	1608	27.40

^a Barrier heights are given in kcal/mol after appropriate ZPVE corrections. The abstracted hydrogen is indicated in boldface.

the bond dissociation energies given in Table 5, the bond strength of the aldehydic C-H bond decreases with increased methyl substitution in the α position, CH₃CH₂CHO > (CH₃)₂-CHCHO > (CH₃)₃CCHO. To a first approximation, every methyl group seems to lower the C(O)-H bond strength by 0.3–0.4 kcal/mol. Similarly the bond strength of the O-H bond in alcohols increases with increasing methyl substitution in the α position (CH₃CH₂OH < (CH₃)₂CHOH < (CH₃)₃COH). The bond strength of the nearly nonpolar vinylic (CHR=CH-H) and secondary vinylic (CH₂=CR---H) bonds decrease as one goes from R equals Et to i-Pr to t-Bu. The magnitude of the decrease is rather small (~0.1 to 0.2 kcal/mol). Of the reactions considered, the weakest bond to be abstracted is the central C-H bond in 1,4-pentadiene. This bond is in an allylic position with respect to two double bonds. Except for the allylic, propargylic, and aldehydic C-H bonds, the rest of the abstraction reactions are either nearly thermoneutral or endothermic.

Derivation of "Supergroup" Thermo Values

In Tables 6 and 7, we present the thermochemical values of the reactive moiety for the individual reactions studied as well as the average for a specific reaction type, "supergroups". A quick glance reveals that the contribution from the reactive

moiety remains essentially the same for all the members despite the significant variation in the reactant structure. The S and Cp(T) values for {CO/C/-H/H}, {O/CO/-H/H}, {O/C/-H/H}, {C_d/H/-H/H}, {C_d/C/-H/H}, and {C/-H/H} are in very good agreement, with a standard deviation of less than 0.25 cal/mol-K. The heats of formation of all "supergroups" display a systematic trend while going from an Et, to i-Pr, to t-Bu substituent. Interestingly, in contrast to H-abstraction from alkanes, one can observe such a trend even in the 0 K barrier height itself. In the case of aldehydes, the $\Delta H_f^{(298\text{K})}$ of the {CO/C/-H/H} group decreases by 0.3 kcal/mol for each additional methyl substitution. In the case of olefins, the {C_d/H/-H/H} enthalpy value decreases by 0.15 kcal/mol, while for {C_d/C/-H/H} the decrease is about 0.3 kcal/mol for each methyl substitution. One observes a similar systematic decrease (0.5 kcal/mol) in $\Delta H_f^{(298\text{K})}$ for the alkynyl H-abstraction, with increased methyl substitution in the carbon α to the alkynyl group.

Inclusion of the reaction from butadiene in the olefin series introduces slightly larger standard deviations for S and Cp(T). As can be observed from Table 6, the Cp(T) values for the reactive moiety derived from the transition state of the reaction CH₂=CHCH=CH₂ + H is slightly smaller in magnitude

TABLE 5: CBS-Q Bond Dissociation Energies of R-H and Heats of Reaction for R-H + H → R• + H₂^a

dissociation reaction	BDE at 0K	ΔH _R	⟨S ² ⟩
HCHO → H + HCO	87.06	-17.39	0.766
CH ₃ CHO → H + CH ₃ CO	87.84	-16.61	0.764
CH ₃ CH ₂ CHO → H + CH ₃ CH ₂ CO	88.29	-16.15	0.764
(CH ₃) ₂ CHCHO → H + (CH ₃) ₂ CHCO	87.97	-16.48	0.764
(CH ₃) ₃ CCHO → H + (CH ₃) ₃ CCO	87.49	-16.95	0.764
			0.000
CH ₃ OH → H + CH ₃ O	104.32	-0.13	0.761
CH ₃ CH ₂ OH → H + CH ₃ CH ₂ O	104.98	0.54	0.759
CH ₃ CH ₂ CH ₂ OH → H + CH ₃ CH ₂ CH ₂ O	104.52	0.07	0.759
(CH ₃) ₂ CHOH → H + (CH ₃) ₂ CHO	105.56	1.11	0.759
(CH ₃) ₃ COH → H + (CH ₃) ₃ CO	105.40	0.95	0.759
			0.000
HC(O)OH → H + HC(O)O	114.38	9.93	0.760
CH ₃ C(O)OH → H + CH ₃ C(O)O	112.73	8.28	0.759
CH ₃ CH ₂ C(O)OH → H + CH ₃ CH ₂ C(O)O	112.73	8.28	0.759
(CH ₃) ₂ CHC(O)OH → H + (CH ₃) ₂ CHC(O)O	112.04	7.60	0.759
			0.000
CH ₂ =CH ₂ → H + CH ₂ =CH	108.92	4.47	0.876
CH ₂ =CHCH ₃ → H + CH ₃ CH=CH	109.74	5.29	0.905
CH ₂ =CHCH ₂ CH ₃ → H + CH ₃ CH ₂ CH=CH	109.98	5.54	0.905
CH ₂ =CHCH(CH ₃) ₂ → H + (CH ₃) ₂ CHCH=CH	109.78	5.33	0.904
CH ₂ =CHC(CH ₃) ₃ → H + C(CH ₃) ₃ CH=CH	109.61	5.17	0.900
CH ₂ =C(CH ₃) ₂ → H + CH=C(CH ₃) ₂	110.42	5.97	0.899
CH ₂ =CHCH=CH ₂ → H + CH=CHCH=CH ₂	110.38	5.94	1.138
CH ₂ =CHCH ₃ → H + CH ₂ =CCH ₃	105.52	1.08	0.891
CH ₂ =CHCH ₂ CH ₃ → H + CH ₂ =CCH ₂ CH ₃	106.08	1.63	0.889
CH ₂ =CHCH(CH ₃) ₂ → H + CH ₂ =CCH(CH ₃) ₂	105.95	1.51	0.886
CH ₂ =CHC(CH ₃) ₃ → H + CH ₂ =CC(CH ₃) ₃	105.81	1.36	0.884
C(CH ₃) ₂ =CH(CH ₃) → H + C(CH ₃) ₂ =C(CH ₃)	106.15	1.70	0.886
CH ₂ =CHCH ₃ → H + CH ₂ =CHCH ₂	84.96	-19.49	0.951
CH ₂ =CHCH ₂ CH ₃ → H + CH ₂ =CHCH(CH ₃)	81.51	-22.93	0.947
CH ₂ =CHCH(CH ₃) ₂ → H + CH ₂ =CHC(CH ₃) ₂	79.97	-24.48	0.942
(CH ₂ =CH) ₂ CH ₂ → H + (CH ₂ =CH) ₂ CH	70.74	-33.71	1.146
HCCCH → H + HCC	130.89	26.44	1.056
CH ₃ CCH → H + CH ₃ CC	133.64	29.19	1.028
CH ₃ CH ₂ CCH → H + CH ₃ CH ₂ CC	132.49	28.04	1.027
(CH ₃) ₂ CHCCH → H + (CH ₃) ₂ CHCC	131.03	26.58	1.026
HCCCH ₃ → H + HCCCH ₂	88.71	-15.74	0.923
HCCCH ₂ CH ₃ → H + HCCCHCH ₃	85.95	-18.50	0.919
HCCCH(CH ₃) ₂ → H + HCCCH(CH ₃) ₂	84.34	-20.10	0.913
CH ₂ =CHCH=CH ₂ → H + CH ₂ =CCH=CH ₂	107.33	2.88	1.098
CH ₂ =CHC(CH ₃)=CH ₂ → H + CH ₂ =CC(CH ₃)=CH ₂	107.33	2.89	1.053
CH ₂ =CHCCH → H + CH ₂ =CCCH	97.17	-7.28	1.207

^a The ⟨S²⟩ value corresponds to the radical R•. The abstracted hydrogen is indicated in boldface.

compared to that from other alkenes. The spin contamination in the transition state is more than in other cases and we therefore doubt the accuracy of the calculated force constants. Though the CBS-Q model chemistry has a correction term for the absolute energy because of spin contamination, the effect of spin-contamination on the calculated force constant matrix is not yet well understood.

In the case of acids, the range of enthalpy values for the reactive moiety (“{O/CO/-H/H}”) is larger than the GAV range for “supergroups” of other reaction types. The effect of methyl substitution is also large and is not systematic. In contrast to some other series, the structural variation occurs not in the β position (R^β-O-H, R^β-C(O)-H, R^β-C(=CH₂)-H) but in the γ position (R^γ-C(O)-O-H) with respect to the abstracting hydrogen. The computed barrier height for H-abstraction from acids (Table 5) varies substantially in what appears to be, a nonsystematic way. Formic acid could be expected to behave differently from other R-COOH groups, because the R group is more electron donating compared to the H group. Furthermore, the formoxy radical has several low-lying electronic states. The UHF/6-31G(d') level of optimization as used in CBS-Q for ZPVE corrections leads to the symmetry broken ²A' state, which is shown by Rauk et al.^{31a} using a high level of CASPT2 and MRCI calculations, to be an excited state. Since

the reaction is slightly endothermic, one can anticipate similar difficulties in calculating the transition state energies especially within the single configuration approach.

As can be observed from Table 5, the C(O)O-H BDE as well as the geometrical parameters of the reactive moiety (Table 4) in acetic and propanoic acids are very nearly the same. However, the barrier height for H-abstraction from propanoic acid is approximately 0.5 kcal/mol lower than those found for the other acids. Although this is well within the error bars of the calculation, the analogy with other series studied herein implies that there might be a systematic decrease of the barrier caused by methyl substitution of the γ carbon. In the case of i-PrCOOH, the calculated barrier height for H-abstraction is even lower (by 1 kcal/mol), but this is partly because of the unique conformation of the transition state. The -C(O)OH group in acid can exhibit two orientations with respect to the CR₃ α group i.e., (i) the C-R group being eclipsed with respect to C=O and (ii) the C-R group being eclipsed with respect to C-OH bond. In all acids other than i-PrCOOH, the favored conformation is (i) i.e., the C=O group of the acid eclipses with one of the α C-H or C-C bonds in both the reactant as well as in the transition structure. This is further supported by the experimental observation on CH₃CHO^{32a} and CH₃COCH₃^{32b} systems wherein the preferred conformation of a CH₃CO group

TABLE 6: Group Additivity Values for Transition State “Supergroups”, Belonging to Hydrogen-Abstraction Reactions from Alkenes and Alkynes by H Atom^a

“supergroup”	reactions	ΔH_f^{298}	S^{298}	c_p^{300}	c_p^{400}	c_p^{500}	c_p^{600}	c_p^{800}	c_p^{1000}	c_p^{1500}
{C _d /H/-H/H}	CH ₂ =CH ₂ + H	71.15	33.08	9.00	11.06	12.67	13.90	15.57	16.65	18.12
	CH ₃ CH=CH ₂ + H	71.43	33.45	8.91	10.75	12.33	13.58	15.33	16.46	18.01
	CH ₃ CH ₂ CH=CH ₂ + H	71.30	33.33	8.87	10.71	12.30	13.56	15.31	16.45	18.01
	(CH ₃) ₂ CHCH=CH ₂ + H	71.14	33.70	8.77	10.65	12.28	13.56	15.32	16.46	18.01
	(CH ₃) ₃ CCH=CH ₂ + H	71.02	33.41	8.80	10.67	12.32	13.65	15.47	16.62	18.13
	(CH ₃) ₂ C=CH ₂ + H	71.50	33.54	8.71	10.40	11.96	13.25	15.08	16.27	17.91
	CH ₂ =CHCH=CH ₂ + H	71.77	33.84	8.98	10.30	11.57	12.80	14.91	16.43	18.54
	average	71.26	33.42	8.84	10.71	12.31	13.58	15.35	16.49	18.03
	std. dev.	0.19	0.21	0.11	0.21	0.22	0.21	0.17	0.14	0.08
	CH ₃ CH=CH ₂ + H	70.77	13.87	7.90	9.30	10.49	11.45	12.81	13.57	14.41
{C _d /C/-H/H}	CH ₃ CH ₂ CH=CH ₂ + H	70.64	13.91	7.77	9.21	10.42	11.39	12.76	13.53	14.39
	(CH ₃) ₂ CHCH=CH ₂ + H	70.28	13.78	7.12	8.88	10.36	11.51	13.02	13.80	14.58
	(CH ₃) ₂ CCH=CH ₂ + H	70.08	13.40	7.72	9.21	10.56	11.68	13.21	14.00	14.73
	(CH ₃)CH=C(CH ₃) ₂ + H	70.53	13.82	7.74	9.05	10.23	11.21	12.62	13.42	14.32
	average	70.46	13.76	7.65	9.13	10.41	11.45	12.88	13.66	14.49
	std. dev.	0.28	0.20	0.30	0.17	0.13	0.17	0.23	0.23	0.17
	CH ₂ =CHCH=CH ₂ + H	70.30	13.01	8.67	9.96	10.95	11.81	13.23	14.18	15.35
	CH ₂ =CHC(CH ₃)=CH ₂ + H	70.18	13.04	7.73	8.95	10.27	11.46	13.20	14.24	15.40
	average	70.24	13.03	8.20	9.46	10.61	11.64	13.22	14.21	15.37
	std. dev.	0.28	0.20	0.30	0.17	0.13	0.17	0.23	0.23	0.17
{C _d /C _d /-H/H}	CH ₃ -CH=CH ₂ + H	46.32	33.51	9.55	12.51	14.97	16.89	19.42	21.02	23.10
	{C/C _d /H ₂ /-H/H}	49.98	13.49	9.19	11.85	13.97	15.52	17.40	18.46	19.65
	{C/C _d /C/H/-H/H}	51.60	-7.64	7.23	10.32	12.54	13.77	15.18	15.74	16.27
	{C/C _d /C ₂ /-H/H}	47.69	11.14	9.58	13.22	15.47	16.81	18.19	18.98	19.81
	{C/C _d 2/H/-H/H}	107.26	32.41	9.40	10.24	10.92	11.49	12.33	12.88	13.57
	HCCH + H	106.88	32.51	8.89	9.76	10.51	11.14	12.10	12.72	13.49
	CH ₃ CCH + H	106.46	32.66	8.92	9.78	10.52	11.16	12.10	12.72	13.49
	CH ₃ CH ₂ CCH + H	105.85	32.93	8.98	9.82	10.55	11.17	12.11	12.72	13.49
	(CH ₃) ₂ CHCCH + H	105.85	32.93	8.98	9.82	10.55	11.17	12.11	12.72	13.49
	average	106.40	32.70	8.93	9.78	10.53	11.16	12.10	12.72	13.49
std. dev.	0.52	0.21	0.05	0.03	0.02	0.01	0.01	0.00	0.00	
{C/C _d /H ₂ /-H/H}	CH ₃ CCH + H	49.16	35.29	9.56	12.06	14.19	15.92	18.37	20.05	22.46
	{C/C _d /C/H/-H/H}	50.65	15.41	8.62	10.76	12.52	13.93	15.92	17.22	18.92
	{C/C _d /C ₂ /-H/H}	50.76	-6.01	7.90	9.86	11.33	12.42	13.89	14.68	15.69
	{C _d /C _d /-H/H}	66.45	14.30	9.55	11.43	12.71	13.53	14.44	14.85	15.20

^a The name of the “supergroup” is given in the first column and the abstracted hydrogen in each reaction is indicated in boldface.

TABLE 7: Group Additivity Values for Transition State “supergroups”, Belonging to Hydrogen-Abstraction Reactions from Alcohols, Aldehydes, and Acids by H Atom^a

“supergroup”	reactions	ΔH_f^{298}	S^{298}	c_p^{300}	c_p^{400}	c_p^{500}	c_p^{600}	c_p^{800}	c_p^{1000}	c_p^{1500}
{CO/H/-H/H}	HCHO + H	29.80	57.44	11.66	13.39	15.01	16.39	18.47	19.87	21.75
	CH ₃ CHO + H	25.28	40.20	10.34	11.76	13.21	14.39	16.11	17.08	
	CH ₃ CH ₂ CHO + H	25.01	40.12	10.00	11.53	13.07	14.30	16.06	17.05	
	(CH ₃) ₂ CHCHO + H	24.71	39.93	10.23	11.78	13.32	14.54	16.26	17.20	
	(CH ₃) ₃ CCHO + H	24.43	39.59	11.18	12.42	13.74	14.83	16.42	17.31	
{CO/C/-H/H}	average	25.00	40.08	10.19	11.69	13.20	14.41	16.14	17.11	
	std. dev.	0.28	0.14	0.18	0.14	0.13	0.12	0.10	0.08	
	HC(O)OH + H	9.09	29.18	6.90	8.87	10.30	11.24	12.52	13.05	
	CH ₃ C(O)OH + H	9.74	29.23	7.06	8.94	10.32	11.27	12.62	13.19	
	CH ₃ CH ₂ C(O)OH + H	9.29	29.10	7.13	9.06	10.44	11.37	12.66	13.20	
{O/CO/-H/H}	(CH ₃) ₂ CHC(O)OH + H	8.22	28.85	7.24	9.06	10.36	11.25	12.57	13.16	
	average	9.08	29.09	7.08	8.98	10.36	11.28	12.59	13.15	
	std. dev.	0.64	0.17	0.14	0.10	0.06	0.06	0.06	0.07	
	CH ₃ OH + H	25.41	33.62	7.19	8.07	9.03	9.81	11.01	11.72	12.39
	CH ₃ CH ₂ OH + H	25.56	33.12	7.18	8.12	9.10	9.88	11.07	11.77	12.41
{O/C/-H/H}	CH ₃ CH ₂ CH ₂ OH + H	25.37	33.23	7.25	8.16	9.11	9.88	11.06	11.75	12.40
	(CH ₃) ₂ CHOH + H	25.37	33.07	7.32	8.31	9.30	10.07	11.21	11.86	12.45
	(CH ₃) ₃ COH + H	24.99	32.89	7.44	8.48	9.43	10.14	11.19	11.81	12.39
	average	25.34	33.19	7.28	8.23	9.19	9.96	11.11	11.78	12.41
	std. dev.	0.21	0.27	0.11	0.17	0.17	0.14	0.09	0.06	0.03

^a The name of the “supergroup” is given in the first column, and the abstracted hydrogen in each reaction is indicated in boldface.

is with the C–H bond being eclipsed with the C=O bond. The equilibrium structure of the *i*-PrCOOH follows this orientation while the preferred conformation in the transition structure corresponds to the case (ii) (discussed above) in contrast to our expectation and is energetically more stable. We consider this system as unique and we excluded this reaction while averaging for ΔH_f (Table 7). It would be worthwhile to have few additional systems in order to average the ΔH value for {O/CO/-H/H}. However, we were not successful in obtaining the CBS–Q

energies for the transition structure from *t*-BuCOOH within our available computational resources.

We have shown in our first paper⁴ that the rate constants calculated using the averaged thermochemical values (“supergroup”) agree within a factor of 2 with TST rates for all individual reactions. Here, we again find that a single “supergroup” value accurately reproduces the TST rates of the individual reactions in every case except for the abstractions from carboxylic acids, where there are special issues detailed above.

TABLE 8: Modified Arrhenius Fitted Parameters for the GA Predicted Rates^a

“supergroup”	A	E_a/R	n	reaction family
{CO/H/-H/H}	5.48×10^7	1.22×10^3	1.82	HCHO + H → HCO + H ₂
{CO/C/-H/H}	8.07×10^7	3.37×10^2	1.76	RCHO + H → RCO + H ₂
{O/C/-H/H}	8.70×10^8	5.05×10^3	1.39	ROH + H → RO + H ₂
{O/CO/-H/H}	3.30×10^8	6.99×10^3	1.56	RCOOH + H → RCOO + H ₂
{C _d /H/-H/H}	2.53×10^7	5.91×10^3	1.98	R ₂ C=CH ₂ + H → R ₂ C=CH + H ₂
{C _d /C/-H/H}	2.98×10^7	4.33×10^3	1.95	RCH=CR ₂ + H → RC=CR ₂ + H ₂
{C/C _d /H2/-H/H}	4.33×10^5	1.41×10^3	2.38	R ₂ C=CRCH ₃ + H → R ₂ C=CRCH ₂ + H ₂
{C/C _d /C/H/-H/H}	6.99×10^5	5.58×10^2	2.36	R ₂ C=CRCH ₂ R + H → R ₂ C=CRCHR + H ₂
{C/C _d /C2/-H/H}	3.02×10^6	-227.30	2.16	R ₂ C=CRCHR ₂ + H → R ₂ C=CRCR ₂ + H ₂
{C/-H/H}	1.30×10^8	1.34×10^4	1.88	RCCH + H → RCC + H ₂
{C/C/H2/-H/H}	2.70×10^7	3.00×10^3	1.91	RCCCH ₃ + H → RCCCH ₂ + H ₂
{C/C/C/H/-H/H}	7.79×10^7	1.06×10^3	1.78	RCCCH ₂ R + H → RCCCHR + H ₂
{C/C/C2/-H/H}	1.21×10^8	-367.10	1.72	RCCCHR ₂ + H → RCCCR ₂ + H ₂
{C/C _d 2/H/-H/H}	7.09×10^3	-951.50	2.85	R ₂ C=CH-CH ₂ -CH=CR ₂ + H → R ₂ C=CH-CH=CH=CR ₂ + H ₂
{C _d /C/-H/H}	2.18×10^6	3.06×10^3	2.40	RCC-CH=CR ₂ + H → RCC-C=CR ₂ + H ₂
{C _d /C _d /-H/H}	1.93×10^8	5.15×10^3	1.74	R ₂ C=CRCH=CR ₂ → R ₂ C=CRC=CR ₂ + H ₂

^a A is given in cm³ mol⁻¹ s⁻¹ and E_a/R in kelvin.

Comparison of the GA Predicted Rate Rule with Literature Estimates

As mentioned in the Introduction, many of the reactions investigated in this work have limited experimental information describing their mechanism and product distributions. In this section, we therefore compare our GA-predicted rates with kinetic information found in the commonly used and well-known modeling reaction sets such as GRIMEch3.0³³ (Gas Research Institute), LLNL³⁴ (Lawrence Livermore National Laboratory), Konnov mechanism,³⁵ Tsang’s prediction,³⁶ Hidaka’s shock tube and modeling works,³⁷ and the NIST kinetic database.³⁸ For some reactions i.e., acid hydrogen ({O/CO/-H/H}), the alkyl-substituted propargylic hydrogen ({C/C_d/C/H/-H/H}, {C/C_d/C2/-H/H}), diallylic hydrogen ({C/C_d2/H/-H/H}, and {C/C_d2/C/-H/H}) abstractions, no rate estimates are available for comparison. The latter two reactions are exothermic and are associated with very small barriers. In Table 8, we present modified Arrhenius rate expressions for these rate constants, since modeling programs such as CHEMKIN³⁹ or CHEMDIS⁴⁰ require this form of input. These Arrhenius expressions were obtained by fitting the $k(T)$ s derived from the GAV of the TS over the range $300 \leq T \leq 1500$ K.

Figure 1 compares the GA-predicted rate for vinylic H-abstraction rates with literature data. All of the low temperature experimental measurements are for radical addition. However, at combustion temperature addition across the double bond is negligible and the measured rate is essentially 100% H-abstraction. The rate expressions used in GRIMEch and Konnov for vinylic hydrogen (Figure 1a) are very similar, while LLNL suggests a much higher rate. It is interesting to note that the ab initio predictions are between these two limits. Also, our results are in excellent agreement with the recommendations of Baulch⁴¹ and the NIST-averaged data. The reaction C₂H₄ + H → C₂H₃ + H₂ is nearly thermoneutral. However, this reaction has a high barrier, and thus experimental data are found only at high temperatures. Figure 1b compares our generic prediction for the vinylic H-abstraction with experimental results for H + ethylene. Although the data show large deviations, we find good agreement with the more recent data. In general, our GA rate is in the midst of all results and appears to be reasonable.

For the abstraction of secondary vinylic hydrogens, RCH=CR’R’’ there are no rate estimates in GRI or Konnov’s mechanism. The LLNL mechanism uses Tsang’s recommendations, which are based on the assumption that the effect of methyl substitution is the same in olefins as it is in alkanes. At temperatures higher than 1000 K, this estimate is a factor of

two lower than that predicted by our GA calculations. Note that this is still within the uncertainty limit estimated by Tsang. There are no direct experimental measurements on the rate expression for the abstraction from the allylic position. Among the available C-H bonds in an olefin, abstraction of the allylic H is the most facile one. All mechanisms (LLNL, NIST, Tsang) use the same recommended value, and our GA estimate for allylic H is a factor of 2.7 higher throughout the temperature range. Surprisingly, the GRI mechanism does not include propene. Additional experimental data are needed to confirm the magnitude of the A factor for this reaction. In summary, the rate predictions presented here are reasonable, but tend to be on the high end of available estimates. The order of reactivity of the hydrogens in the olefin series (Figure 2) toward abstraction reaction (diallylic > disubstituted allylic > monosubstituted allylic > allylic > secondary vinylic > vinylic) is in accordance with the relative stability of the resulting radicals and general expectation based on intuition.

Alkynyl C-H bonds are very strong (BDE > 131 kcal/mol), so the reverse reaction, RCC + H₂, is very exothermic and has a low barrier. Because of the low barrier, tunneling is relatively unimportant. Compared to olefins, alkynes are less susceptible to addition reactions. A quick look at Figure 3a shows the large range of values that are being used by modelers for this abstraction rate. Often, they use the simple Arrhenius rate expression. The fitted-rate expression from the NIST experimental database lies above the recent experimental work on C₂H₂ by Peeters et al.⁴² We found only two sets of direct experimental data for this reaction. Most of the experimental investigations are indirect and are deduced from the thermodynamic and the rate constant data for the reverse reaction, H₂ + C₂H → H + C₂H₂. However, for the C₂H radical, the literature values on heats of formation vary from 114.0 to 135.0 kcal/mol (Chase,⁴³ 114.0; Benson,^{1a} 122 ± 3; Tsang,⁴⁴ 33 ± 2; Bozelli,²⁸ 134.46; and Golden,⁴⁵ 134.79 ± 0.96 kcal/mol). There is also uncertainty with respect to its entropy for which values in the range of 49.58 to 50.6 cal/mol-K can be found. The calculated ΔH_f^{298} value at the CBS-Q level of theory equals 136.0 kcal/mol, with S^{298} being 50.16 cal/mol-K. Herein we compute the forward reaction (C₂H₂ + H) rate by combining the experimental rate for the reverse reaction with ab initio based thermodynamic data of the C₂H radical. To verify the reliability of the latter data, we calculated the rate for the C₂H + H₂ reaction and compared it with the experimentally derived value tabulated in the NIST database. This comparison showed an excellent agreement with experimental data over the whole range

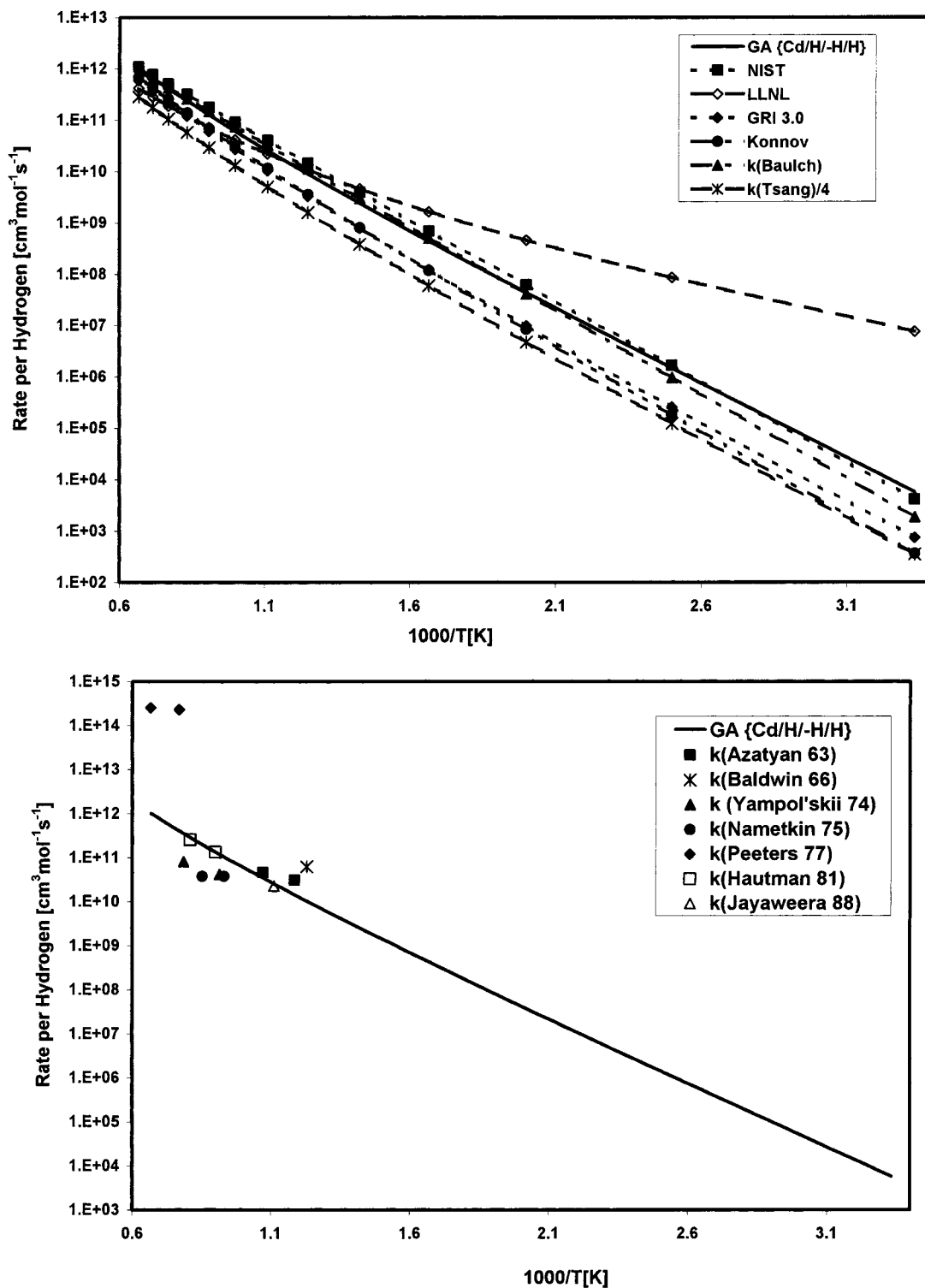


Figure 1. (a) Comparison of group additivity predicted rates for olefinic H-abstraction with literature. References: NIST data are based on ref 38; GRI mech, ref 33; LLNL, ref 34; Konnov, ref 35; Tsang, ref 36; and Baulsch, ref 40. References 33, 36, and 40 correspond to the reaction, $\text{C}_2\text{H}_4 + \text{H}$. The group-additivity predictions lie between the estimates used in modeling studies. (b) Comparison of the group additivity predicted generic rate for H-abstraction from ethylene with experimental rates. ■ (ref 51), * (ref 52), ▲ (ref 53), ● (ref 54), ◆ (ref 55), □ (ref 56), △ (ref 57).

of T ($300 \leq T \leq 1500 \text{ K}$), giving us confidence in the C_2H ab initio data. Figure 3b portrays the comparison of our generic rate for alkynyl H-abstraction with both the direct experimental results on the $\text{C}_2\text{H}_2 + \text{H}$ reaction and the indirect rates based on $k^{\text{exp}}(T)$ for the $\text{C}_2\text{H} + \text{H}_2$ reaction. The GA prediction is found between the range of reference rates.

Not much is known about the propargylic C–H abstraction rates, and our predictions based on quantum chemical calculations stand as sole theoretical estimates. As observed among

the substituted allylic C–H abstraction, the reactivity of the propargylic C–H bond toward abstraction increases with alkyl substitutions i.e., disubstituted propargylic > monosubstituted propargylic > propargylic.

In the case of alcohols, R–OH, the hydrogen atom can abstract from either the O–H hydrogen or one of the hydrogens of the R group. The former abstraction is few kcal/mol more endothermic than the latter because of the relative bond strengths of the O–H and C–H bonds. Experimental detection⁴⁶ and

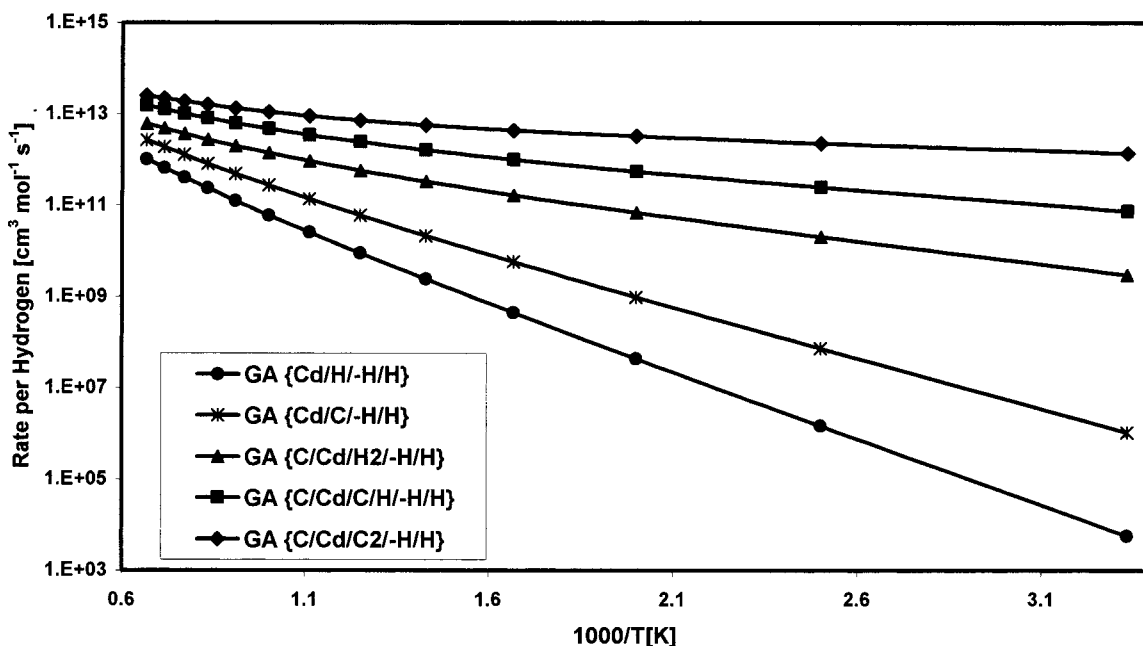


Figure 2. Group additivity predicted rates for H-abstraction reactions of different types of hydrogen in alkenes.

calibration of CH_2OH and CH_3O radicals from the $\text{H} + \text{CH}_3\text{OH} \rightarrow \text{CH}_3\text{O}/\text{CH}_2\text{OH} + \text{H}_2$ reaction is difficult because of the fast secondary reaction, $\text{H} + \text{CH}_3\text{O}/\text{CH}_2\text{OH} \rightarrow \text{products}$. The results obtained at lower temperatures are not in line with the high-temperature expression derived from shock-tube measurements. The experimental values of the branching ratio for the reaction channels (a) $\text{CH}_3\text{O} + \text{H}_2$ and (b) $\text{CH}_2\text{OH} + \text{H}_2$ are uncertain, contradictory, and temperature dependent. Recent theoretical studies of Lendvay et al.^{47a} and Jodkowski et al.^{47b} have revealed that the CH_2OH formation is the dominant reaction channel, contributing over 95% of the overall reaction below 1200 K. At low temperatures there is an appreciable contribution to the rate constant via quantum mechanical tunneling. Lendvay et al. also calculated the barrier height for the abstraction by H from the OH group of methanol at PMP2/6-311G**//MP2/6-311G**, MP4SDTQ/6-311G**//MP2/6-311G**, G2MP2, G1, and G2 levels. At all levels of treatment, abstraction from the OH hydrogen is found to involve a higher-energy pathway as compared to the abstraction from the alkyl group of the alcohols, ROH. At the best level of their treatment, G2, the calculated barrier height is 14.1 kcal/mol. This is nearly 2 kcal/mol higher than the value computed in the present work at the CBS-Q level. No experimental estimate is available for the barrier height of this reaction. Nevertheless, our calculated rate is lower than the experimentally observed total rate for H-abstraction from methanol.

Reactions of aldehydes with a H atom could proceed either via a direct abstraction or by an initial addition of H to either the oxygen or the carbon end of the $\text{C}=\text{O}$ group, followed by various reactions or collisional quenching of the chemically activated adduct. Usually the direct abstraction channel is regarded as the dominant channel because of the low C-H bond energy in aldehydes. Hence, one can expect that the experimental total rate for $\text{H} + \text{HCHO} \rightarrow \text{H}_2 + \text{HCO}$ is close to the direct abstraction rate. In Figure 4a, we compare our GA prediction with some selected experimental data. Wagner et al.⁴⁸ have investigated the rate constants and product distributions of abstraction and addition reactions of HCHO with H in the temperature range $296 \text{ K} \leq T \leq 780 \text{ K}$ at pressures of few millibars using the discharge flow method with electron paramagnetic resonance (EPR) for the detection of H and D

atoms, and laser-induced fluorescence (LIF) for the measurement of HCO. The overall rate constant was determined using the pseudo-first-order method with $[\text{HCHO}] \gg [\text{H}]$. The Arrhenius expression for the experimental abstraction rate constant is $(8.7 \pm 1.9) \times 10^{12} \exp[(-14.5 \pm 0.7) \text{ kJ mol}^{-1}/RT]$. Although the experimental rates presented are based on measurements, owing to the severe impacts of side reactions these data are extracted after additional modeling studies. Figure 4a shows a large scatter of the experimental data with our predictions being slightly higher than the measured data with a good agreement for the temperature dependence. The calculated rate of $2.9 \times 10^{10} \text{ cm}^3/\text{mol}\cdot\text{s}$ at 300 K is in reasonable agreement with the experimental results of Wagner et al.,⁴⁸ $1.2 \times 10^{10} \text{ cm}^3/\text{mol}\cdot\text{s}$. The low-temperature discrepancies observed here as well as in our earlier work⁴ on abstraction by H from alkanes suggest that CBS-Q calculations tend to underestimate the barrier height for abstraction reactions by H. The simple tunneling treatment used in this work is known to underestimate contributions from tunneling when compared to sophisticated improved treatments such as multidimensional, centrifugal, dominant-small-curvature⁴⁹ methods. Thus, application of these methods would probably not improve the agreement between the calculated and experimental reaction rates. At high Ts the GA-predicted rate is in excellent agreement with Hidaka's et al.⁵⁰ shock tube studies. Figure 4b shows a comparison with some rate estimates used in the literature models. Interestingly, the rate used in the GRI3.0 mechanism shows a significantly different temperature dependence compared with all other predictions.

The limited experimental rate data and the relatively large uncertainties in the thermochemistry of several of the product radicals make it difficult to estimate the accuracy of the calculations presented in this work. Because of the increased electron correlation and spin-contamination problems with unsaturated radicals and TSs, the estimates here are not as certain as the very accurate (\sim a factor of 2) estimates presented for reactions involving alkanes in the first paper of this series. Golden et al.⁶³ investigated the accuracy of barrier height predictions from different quantum chemical methods in conjunction with different treatments to incorporate tunneling effects. They suggest a procedure to fit the extant experimental data by varying the barrier heights using the calculated partition

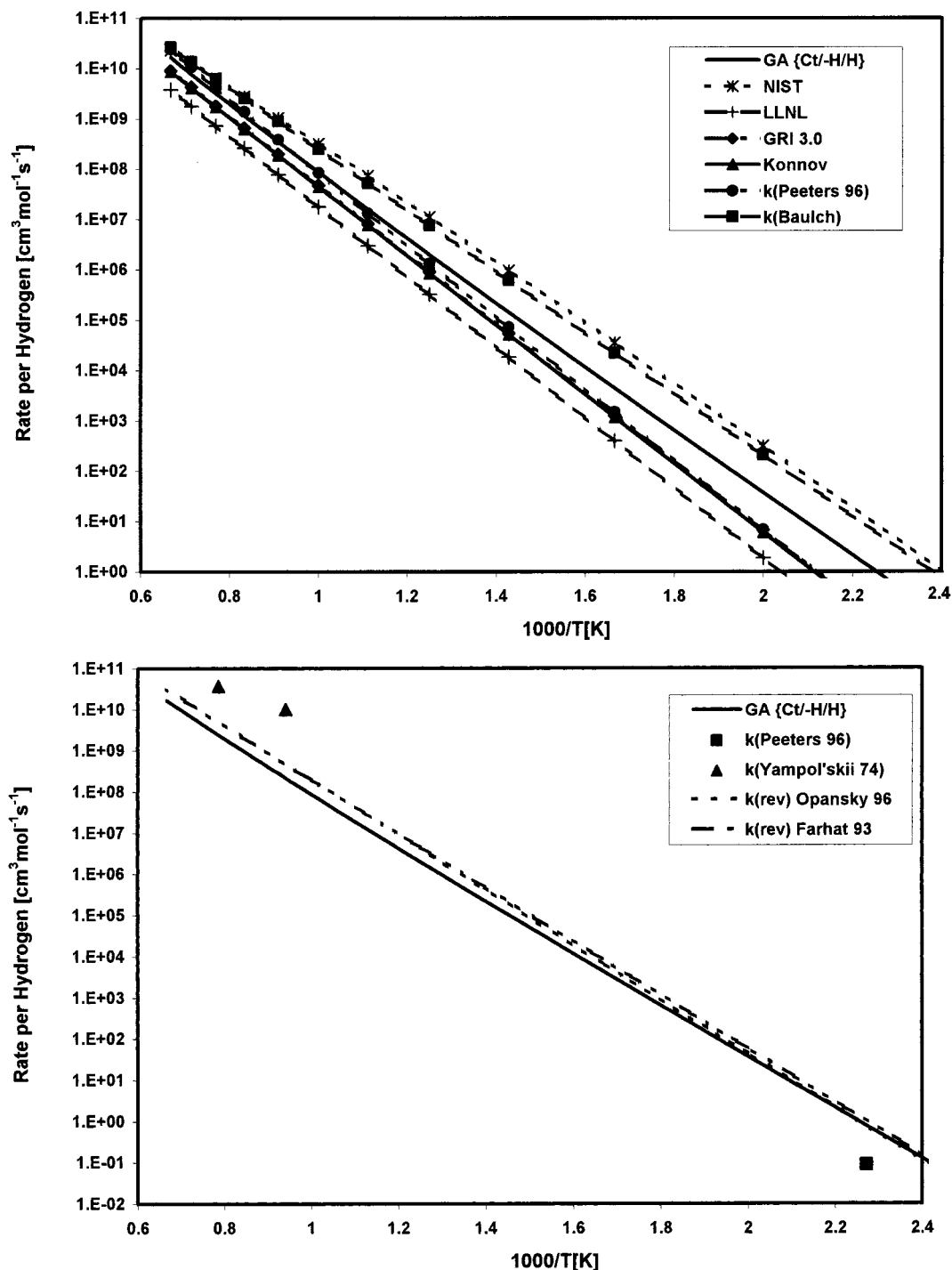


Figure 3. (a) Comparison of group additivity predicted rates for alkynyl H-abstraction reactions with literature. References: NIST data are based on ref 38; GRI mech, ref 33; LLNL, ref 34; Konnov, ref 35; Peeters, ref 42; and Baulsch, ref 40. References 33, 40, and 42 correspond to the reaction $\text{C}_2\text{H}_2 + \text{H}$. The group additivity predictions lie between the estimates used in modeling studies. (b) Comparison of the group additivity predicted generic rate for H-abstraction from acetylene with experimental rates and with rates calculated from $k^{\text{exp}}(T)$ of the reverse reaction, $\text{C}_2\text{H} + \text{H}_2$, based on ab initio thermochemistry for the C_2H radical. ■ (ref 42) and ▲ (ref 57). The solid and varying dashed lines correspond to refs 58 and 59, respectively.

functions and tunneling corrections. However, in the absence of enough experimental kinetic data, it is hard to decide about the accuracy and error bars of our rate predictions. Nonetheless, in every case where experimental data is available, the present estimates appear to have acceptable accuracy.

Conclusions

The structures of nearly 40 transition states corresponding to H-abstraction from systems containing unsaturated double

and triple bonds have been identified and characterized at the CBS-Q level of calculation. The computed thermodynamic properties of the transition state are partitioned into contributions from reactive and unreactive moieties. The contribution of the unreactive moiety is treated to be the same in the reactant and the corresponding transition state and is calculated based on Benson's group values. Investigations on several reactions of the same class, with significant structural variations in the reactant, revealed the thermochemical contribution from the

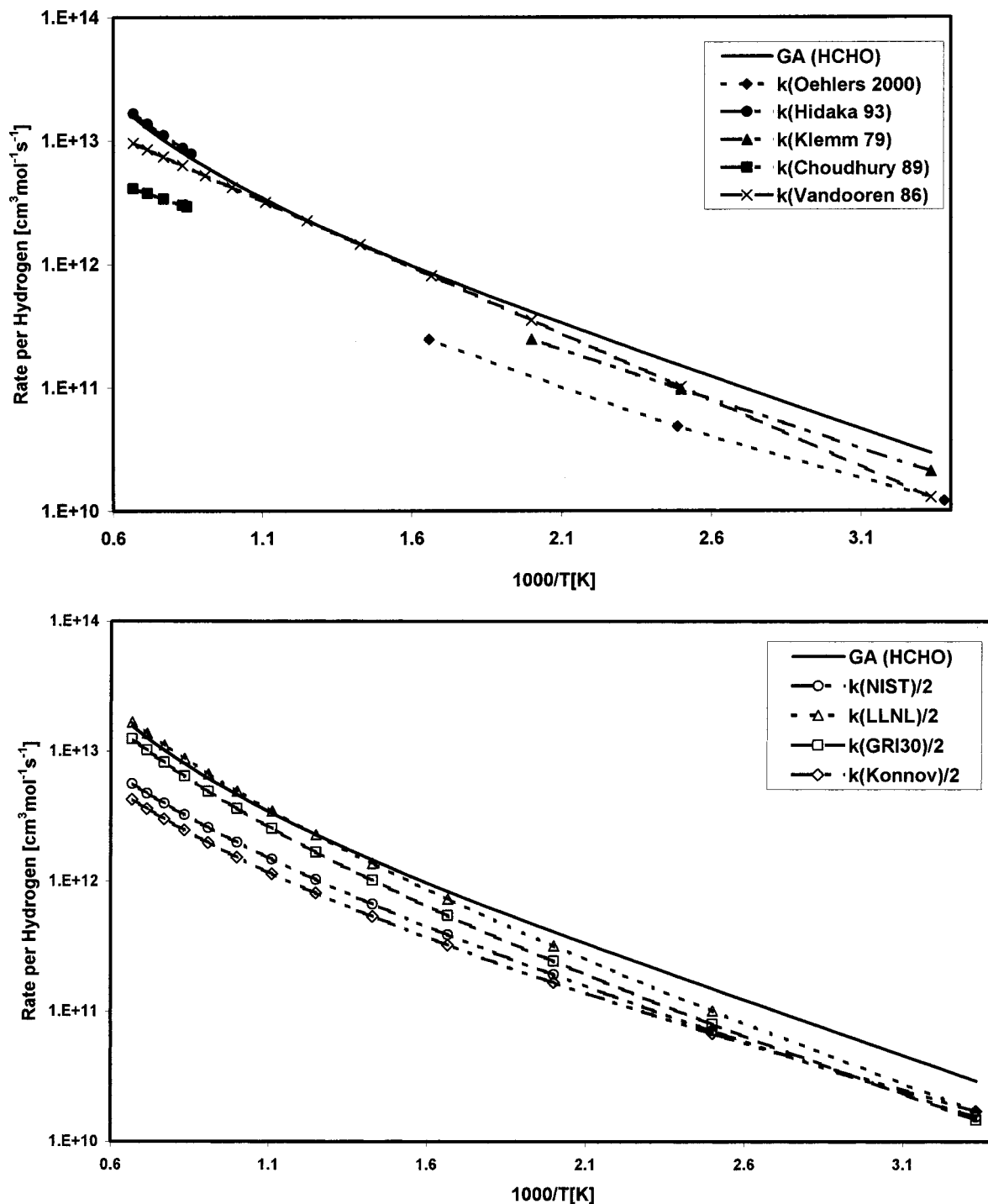


Figure 4. (a) Comparison of the group additivity predicted generic rate for H-abstraction from formaldehyde with experimental rates. \blacklozenge (ref 48) \bullet (ref 50) \blacktriangle (ref 60) \blacksquare (ref 61) and \times (ref 62). (b) Comparison of the group additivity predicted rate for H-abstraction from HCHO with literature data. References: NIST data are based on ref 38; GRImech, ref 33; LLNL, ref 34; Konnov, ref 35; Tsang, ref 36; Hidaka, ref 37; and Baulsch, ref 40. The group additivity prediction lies between the estimates used in modeling studies.

reactive moiety to be nearly constant. The only exception is for abstraction from carboxylic acids, where there are special difficulties discussed above. The “reactive moiety” is then identified with a ‘supergroup’ containing many polyvalent atoms. The $\Delta H_f^{(298)}$ value for several ‘supergroups’ shows small (<0.3 kcal/mol) but systematic variation with increasing methyl substitution in the α position and this parallels the strength of the abstracting bond. Though the magnitude of this energy decrement is very small, and as such within the uncertainty of CBS-Q calculations,²² its consistent occurrence in all the series

studied here allures one to ascribe it to a substituent effect. Work is in progress to definitely identify and estimate substituent effects, if any, in a series of H-abstractions from the alkyl group of the sets (i) R-OH, R-O-R’ and R-OC(O)R’, (ii) R-C(O)H, RC(O)R’, RC(O)OH, RC(O)X, RC(O)OR’ resulting from variations in the group attached, respectively, to the α O and C(O) group. The averaged $\Delta H_f^{(298)}$ neglecting the small substituent effect seem to be accurate enough for most modeling purposes. The 15 new reaction family rate estimation rules derived here should prove very useful in developing new kinetic models.

Acknowledgment. This work was partially supported by National Computational Science Alliance under Grants CHE000004N and CHE000021N and utilized the Exemplar X-Class High-Performance Computing and UniTree Mass Storage Systems. We are grateful for financial support from the EPA Center for Airborne Organics, the NSF CAREER program, Alstom Power, Dow Chemical, and the Division of Chemical Sciences, Office of Basic Energy Sciences, Office of Energy Research, and U.S. Department of Energy through grant DE-FG02-98ER14914.

Supporting Information Available: MP2/6-31G(d') optimized geometries, unscaled harmonic frequencies in (cm⁻¹), and rotational constants (in GHz) of the transition structures. This material is available free of charge via the Internet at <http://pubs.acs.org>.

References and Notes

- Benson, S. W. *Thermochemical Kinetics*, 2nd ed.; Wiley-Interscience: NY, 1976. (b) Cohen, N. *Int. J. Chem. Kinet.* **1982**, *14*, 1339. Cohen, N. *Int. J. Chem. Kinet.* **1983**, *15*, 503. Cohen, N. *Int. J. Chem. Kinet.* **1991**, *23*, 683. Cohen, N. *Int. J. Chem. Kinet.* **1991**, *23*, 397.
- Willems, P. A.; Froment, G. F. *Ind. Eng. Chem. Res.* **1988**, *27*, 1959.
- Willems, P. A.; Froment, G. F. *Ind. Eng. Chem. Res.* **1988**, *27*, 1967.
- Sumathi, R.; Carstensen, H.-H.; Green, W. H., Jr. *J. Phys. Chem. A* **2001**, *105*, 6910.
- Chinnick, S. J.; Baulch, D. L.; Ayscough, P. B. *Chemom. Intell. Lab. Syst.* **1988**, *5*, 39.
- Haux, L.; Cunin, P.-Y.; Griffiths, M.; Come, G.-M. *J. Chim. Phys.* **1988**, *85*, 739.
- Chevalier, C.; Warnatz, J.; Melenk, H. *Ber. Bunsen-Ges. Phys. Chem.* **1990**, *94*, 1362.
- Dente, M.; Pierucci, S.; Ranzi, E.; Bussant, G. *Chem. Eng. Sci.* **1992**, *47*, 2629.
- Chevalier, C.; Pitz, W. J.; Warnatz, J.; Westbrook, C. K.; Melenk, H. *Proc. Combust. Inst.* **1992**, *24*, 93.
- Blurock, E. S. *J. Chem. Inf. Comput. Sci.* **1995**, *35*, 607.
- Nehse, M.; Warnatz, J.; Chevalier, C. *Symp. (Int.) Combust., [Proc.]* **1996**, *26*, 773.
- Ranzi, E.; Faravelli, T.; Gaffuri, P.; Sogaro, A. *Combust. Flame* **1995**, *102*, 179.
- Ranzi, E.; Sogaro, A.; Gaffuri, P.; Pennati, G.; Westbrook, C. K.; Pitz, W. *Combust. Flame* **1994**, *99*, 201.
- Susnow, R. G.; Dean, A. M.; Green, W. H.; Peczak, P. *J. Phys. Chem. A* **1997**, *101*, 3731.
- Broadbelt, L. J.; Start, S. M.; Klein, M. T. *Comput. Chem. Eng.* **1996**, *20*, 113.
- Broadbelt, L. J.; Stark, S. M.; Klein, M. T. *Ind. Eng. Chem. Res.* **1995**, *34*, 2566.
- Broadbelt, L. J.; Stark, S. M.; Klein, M. T. *Ind. Eng. Chem. Res.* **1994**, *33*, 790.
- Frisch, M. J.; Trucks, G. W.; Schlegel, H. B.; Scuseria, G. E.; Robb, M. A.; Cheeseman, J. R.; Zakrzewski, V. G.; Montgomery, J. A.; Stratmann, R. E.; Burant, J. C.; Dapprich, S.; Millam, J. M.; Daniels, A. D.; Kudin, K. N.; Strain, M. C.; Farkas, O.; Tomasi, J.; Barone, V.; Cossi, M.; Cammi, R.; Mennucci, B.; Pomelli, C.; Adamo, C.; Clifford, S.; Ochterski, J.; Petersson, G. A.; Ayala, P. Y.; Cui, Q.; Morokuma, K.; Malick, D. K.; Rabuck, A. D.; Raghavachari, K.; Foresman, J. B.; Cioslowski, J.; Ortiz, J. V.; Baboul, A. G.; Stefanov, B. B.; Liu, G.; Liashenko, A.; Piskorz, P.; Komaromi, I.; Gomperts, R.; Martin, A. L.; Fox, D. J.; Keith, T.; Al-Laham, M. A.; Peng, C. Y.; Nanayakkara, A.; Challacombe, M.; Gill, P. M. W.; Johnson, B.; Chen, W.; Wong, M. W.; Andres, J. L.; Gonzalez, C.; Head-Gordon, M.; Replogle, E. S.; Pople, J. A. *Gaussian 98*, revision A.9; Gaussian, Inc.: Pittsburgh, PA, 1998.
- Montgomery, J. A., Jr.; Ochterski, J. W.; Petersson, G. A. *J. Chem. Phys.* **1994**, *101*, 5900. Ochterski, J. W.; Petersson, G. A.; Montgomery, J. A., Jr. *J. Chem. Phys.* **1996**, *104*, 2598.
- Nicolaidis, A.; Rauk, A.; Glukhovtsev, M. N.; Radom, L. *J. Phys. Chem.* **1996**, *100*, 17460.
- Curtiss, L. A.; Raghavachari, K.; Redfern, P. C.; Pople, J. A. *J. Chem. Phys.* **1997**, *106*, 1063.
- Petersson, G. A.; Malick, D. K.; Wilson, W. G.; Ochterski, J. W.; Montgomery, J. A., Jr.; Frisch, M. J. *J. Chem. Phys.* **1998**, *109*, 10570 and references therein.
- Scott, A. P.; Radom, L. *J. Phys. Chem. A* **1996**, *102*, 16502.
- Atkins, P. W. *Physical Chemistry*, 5th ed.; Oxford University Press: Oxford, **1994**.
- Hirschfelder, J. O.; Wigner, E. *J. Chem. Phys.* **1939**, *7*, 616.
- (a) NIST Webbook, <http://webbook.nist.gov>. (b) *NIST Standard Reference Database 25, Structure and Properties*, version 2.02; January 1994.
- (a) Stull, D. R.; Westrum, E. F., Jr.; Sinke, G. C. *The Chemical Thermodynamics of Organic Compounds*; Krieger Publ. Co.: Malabar, Florida, 1987. (b) Orlov, Y. D.; Lebedev, Y. A. *Russian J. Phys. Chem.* **1991**, *65*, 289. (c) O'Neal, H. E.; Benson, S. W. In *Free Radicals*; Kochi, K., Ed.; Wiley: New York, 1973; Vol. II, p 275. (d) Pedley, J. B.; Naylor, R. D.; Kirby, S. P. *Thermochemical Data of Organic Compounds*, 2nd ed.; Chapman and Hall: New York, 1986.
- Ritter, E. R.; Bozzelli, J. W. *Int. J. Chem. Kin.* **1991**, *23*, 767.
- DeTar, DeL. F. *J. Phys. Chem. A* **1999**, *103*, 7055. DeTar, DeL. F. *J. Phys. Chem. A* **2001**, *105*, 2073.
- Blowers, P.; Masel, R. I. *Theor. Chem. Acc.* **2000**, *105*, 46. Truong, T. N. *J. Chem. Phys.* **2000**, *113*, 4957.
- (a) Rauk, A.; Yu, D.; Borowski, P.; Roos, B. *Chem. Phys.* **1995**, *197*, 73. (b) Haworth, N. L.; Smith, M. H.; Backsay, G. B.; Mackie, J. C. *J. Phys. Chem. A* **2000**, *104*, 7600.
- (a) Mckean, D. C. *Chem. Soc. Rev.* **1978**, *7*, 399 and references therein. (b) Nelson, R.; Pierce, L. *J. Mol. Spectrosc.* **1965**, *18*, 344. Swalen, J. D.; Costain, C. C. *J. Chem. Phys.* **1959**, *31*, 1562. Bowers, P.; Schafer, L. *J. Mol. Struct.* **1980**, *69*, 233.
- Smith, G. P.; Golden, D. M.; Frenklach, M.; Moriarty, N. W.; Eiteneer, B.; Goldenberg, M.; Bowman, C. T.; Hanson, R. K.; Song, S.; Gardiner, W. C., Jr.; Lissianski, V. V.; Qin, Z. *GRIMech 3.0*; http://www.me.berkeley.edu/gri_mech/.
- Curran, H. J.; Gaffuri, P.; Pitz, W. J.; Westbrook, C. K. *Combust. Flame* **1998**, *114*, 149.
- Konnov, A. A. *Detailed reaction mechanism for small hydrocarbons combustion. Release 0.5*; <http://homepages.vub.ac.be/~akonnov/>, 2000.
- Tsang, W. *J. Phys. Chem. Ref. Data* **1991**, *20*, 221.
- Hidaka, Y.; Nishimori, T.; Sato, K.; Henmi, Y.; Okuda, R.; Inami, K. *Combust. Flame* **1999**, *117*, 755. Sato, K.; Hidaka, Y. *Combust. Flame* **2000**, *122*, 291. Hidaka, Y.; Hattori, K.; Okuno, T.; Inami, K.; Abe, T.; Koike, T. *Combust. Flame* **1996**, *107*, 401. Hidaka, Y.; Nakamura, T.; Tanaka, H.; Jinno, A.; Kawano, H.; Higashihara, T. *Int. J. Chem. Kinet.* **1992**, *24*, 761.
- NIST Chemical Kinetics Database*, version 2Q98; Standard Reference Data Program: NIST, MD-20899.
- CHEMKIN, <http://www.ReactionDesign.com>.
- Chang, A. Y.; Bozzelli, J. W.; Dean, A. M. *Z. Phys. Chem.* **2000**, *214*, 1533.
- Baulch, D. L.; Cobos, C. J.; Cox, R. A.; Esser, C.; Frank, P.; Just, Th.; Kerr, J. A.; Pilling, M. J.; Troe, J.; Walker, R. W.; Warnatz, J. *J. Phys. Chem. Ref. Data* **1992**, *21*, 411. Baulsch, D. L.; Cobos, C. J.; Cox, R. A.; Frank, P.; Hayman, G.; Just, Th.; Kerr, J. A.; Murrells, T.; Pilling, M. J.; Troe, J.; Walker, R. W.; Warnatz, J. *J. Phys. Chem. Ref. Data* **1994**, *23*, 847.
- Peeters, J.; Van Look, H.; Ceursters, B. *J. Phys. Chem. A* **1996**, *100*, 15124.
- Chase, M. W., Jr. *NIST-JANAF Thermochemical Tables*, 4th ed.; J. Phys. Chem. Ref. Data, Monograph 9; American Chemical Society: Washington, DC, and American Institute of Physics for the National Institute of Standards and Technology: New York, 1998; p 1.
- Tsang, W. *Energetics of Organic Free Radicals*; Martinho Simoes, J. A., Greenberg, A., Liebman, J. F., Eds.; Blackie Academic and Professional: London, 1996; 22.
- McMillen, D. F.; Golden, D. M. *Annu. Rev. Phys. Chem.* **1982**, *33*, 493.
- (a) Hoyermann, K.; Sievert, R.; Wagner, H. Gg. *Ber. Bunsen-Ges. Phys. Chem.* **1981**, *85*, 149. (b) Meagher, J. F.; Kim, P.; Lee, J. H.; Timmons, R. B. *J. Phys. Chem.* **1974**, *78*, 2650. (c) Spindler, K.; Wagner, H. Gg. *Ber. Bunsen-Ges. Phys. Chem.* **1983**, *86*, 2.
- (a) Lendvay, G.; Berces, T.; Marta, F. *J. Phys. Chem. A* **1997**, *101*, 1588. (b) Jodkowski, J. T.; Rayez, M.-T.; Rayez, J.-C.; Berces, T.; Dobe, S. *J. Phys. Chem. A* **1999**, *103*, 3750.
- Dobe, S.; Oehlers, C.; Temps, F.; Wagner, H. Gg.; Ziemer, H. *Ber. Bunsen-Ges. Phys. Chem.* **1994**, *98*, 754. Oehlers, C.; Wagner, H. Gg.; Ziemer, H.; Temps, F.; Dobe, S. *J. Phys. Chem. A* **2000**, *104*, 10500.
- Truhlar, D. G.; Garrett, B. C. *Annu. Rev. Phys. Chem.* **1984**, *35*, 159. Lu, D. H.; Truong, T. N.; Melissas, V. S.; Lynch, G. C.; Liu, V. P.; Garrett, B. C.; Steckler, R.; Isaacson, A. D.; Rai, S. N.; Hancock, G. C.; Lauderdale, J. G.; Joseph, T.; Truhlar, D. G. *Comput. Phys. Comm.* **1992**, *71*, 235.
- Hidaka, Y.; Taniguchi, T.; Tanaka, H.; Kamesawa, T.; Inami, K.; Kawano, H. *Combust. Flame* **1993**, *92*, 365.
- Azatyay, V. V.; Nalbandyan, A. B.; Ts'ui, M.-Y. *Dokl. Akad. Nauk USSR* **1963**, *149*, 1095.
- Baldwin, R. R.; Simmons, R. F.; Walker, R. W. *Trans. Faraday Soc.* **1966**, *62*, 2486.
- Yampol'skii, Yu. P. *Kinet. Catal.* **1974**, *15*, 938.

- (54) Nametkin, N. S.; Shevel'kova, L. V.; Kalinenko, R. A. *Dokl. Chem. (Engl. Transl.)* **1975**, 221, 851.
- (55) Peeters, J. *Symp. Int. Combust. Proc.* **1977**, 16, 969.
- (56) Hautman, D. J.; Santoro, R. J.; Dryer, F. L.; Glassman, I. *Int. J. Chem. Kinet.* **1981**, 13, 149.
- (57) Yampol'skii, Yu. P.; Lavrovskii, K. P.; Maksimov, Yu. V.; Rybin, V. M. *Kinet. Catal.* **1974**, 15, 17.
- (58) Opansky, B. J.; Leone, S. R. *J. Phys. Chem.* **1996**, 100, 19904.
- (59) Farhat, S. K.; Morter, C. L.; Glass, G. P. *J. Phys. Chem.* **1993**, 97, 12789.
- (60) Klemm, R. B. *J. Chem. Phys.* **1979**, 71, 1987.
- (61) Choudhury, T. K.; Lin, M. C. *Combust. Sci. Technol.* **1989**, 64, 19.
- (62) Vandooren, J.; Oldenhove de Guertechin, L.; van Tiggelen, P. J. *Combust. Flame* **1986**, 64, 127.
- (63) Senosiain, J. P.; Musgrave, C. B.; Golden, D. M. *J. Phys. Chem. A* **2001**, 105, 1669.